

Intracellular pH Regulation in the Renal Proximal Tubule of the Salamander

Basolateral HCO₃⁻ Transport

WALTER F. BORON and EMILE L. BOULPAEP

From the Department of Physiology, Yale University School of Medicine, New Haven, Connecticut 06510

ABSTRACT We have used pH-, Na-, and Cl-sensitive microelectrodes to study basolateral HCO₃⁻ transport in isolated, perfused proximal tubules of the tiger salamander *Ambystoma tigrinum*. In one series of experiments, we lowered basolateral pH (pH_b) from 7.5 to 6.8 by reducing [HCO₃⁻]_b from 10 to 2 mM at a constant pCO₂. This reduction of pH_b and [HCO₃⁻]_b causes a large (~0.35), rapid fall in pH_i as well as a transient depolarization of the basolateral membrane. Returning pH_b and [HCO₃⁻]_b to normal has the opposite effects. Similar reductions of luminal pH (pH_l) and [HCO₃⁻]_l have only minor effects. The reduction of [HCO₃⁻]_b and pH_b also produces a reversible fall in a_i^{Na}. In a second series of experiments, we reduced [Na⁺]_b at constant [HCO₃⁻]_b and pH_b, and also observed a rapid fall in pH_i and a transient basolateral depolarization. These changes are reversed by returning [Na⁺]_b to normal. The effects of altering [Na⁺]_l in the presence of HCO₃⁻, or of altering [Na⁺]_b in the nominal absence of HCO₃⁻, are substantially less. Although the effects on pH_l and basolateral membrane potential of altering either [HCO₃⁻]_b or [Na⁺]_b are largely blocked by 4-acetamido-4-isothiocyanostilbene-2,2'-disulfonate (SITS), they are not affected by removal of Cl⁻, nor are there accompanying changes in a_i^{Cl} consistent with a tight linkage between Cl⁻ fluxes and those of Na⁺ and HCO₃⁻. The aforementioned changes are apparently mediated by a single transport system, not involving Cl⁻. We conclude that HCO₃⁻ transport is restricted to the basolateral membrane, and that HCO₃⁻ fluxes are linked to those of Na⁺. The data are compatible with an electrogenic Na/HCO₃ transporter that carries Na⁺, HCO₃⁻, and net negative charge in the same direction.

INTRODUCTION

There is considerable evidence from experiments on intact renal tubules supporting a linkage between acid secretion and Na⁺ reabsorption in the proximal tubule (see Warnock and Rector, 1979, for a review). Studies on brush-border (i.e., luminal) membrane vesicles prepared from renal tubules

Address reprint requests to Dr. Walter F. Boron, Dept. of Physiology, Yale University School of Medicine, 333 Cedar St., P.O. Box 3333, New Haven, CT 06510.

have identified a Na-H exchanger (Murer et al., 1976), sensitive to amiloride (Kinsella and Aronson, 1980), with attributes consistent with the long-hypothesized luminal Na-H exchanger. In the first paper of this series (Boron and Boulpaep, 1983), we used ion-sensitive microelectrodes and isolated, perfused proximal tubules of the salamander to study, for the first time, Na-H exchange in intact epithelial cells. We found that the salamander proximal-tubule cells indeed possess a luminal Na-H exchanger. Quite unexpectedly, we found that these cells possess a Na-H exchanger at the basolateral membrane as well. Both luminal and basolateral Na-H exchangers serve to regulate intracellular pH (pH_i), much as do comparable transport mechanisms in nerve and muscle cells. The properties of the luminal Na-H exchanger would also enable it to participate in acid secretion. The basolateral Na-H exchanger, however, is physiologically oriented in the wrong direction to effect the basolateral uptake of acid necessary for transcellular acid secretion.

In view of the HCO_3^- dependence of proximal-tubule acid secretion (see Warnock and Rector, 1979), it has long been supposed that the basolateral step in acid secretion is actually brought about by the exit of HCO_3^- . Until now, the most direct evidence for basolateral HCO_3^- transport came from the studies of Frömter and his colleagues (Frömter, 1975; Burckhardt and Frömter, 1980), who inferred a HCO_3^- or OH^- conductance from transient changes in basolateral membrane potential, and those of Ullrich and his colleagues (Radtke et al., 1972; Ullrich et al., 1971, 1975, 1977), who studied the reabsorption of non- HCO_3^- buffers.

The aforementioned studies, however, have not provided unambiguous evidence for basolateral HCO_3^- transport. We now report a direct study of basolateral HCO_3^- transport in which we used isolated, perfused proximal tubules of the tiger salamander *Ambystoma tigrinum* together with microelectrodes for measuring cell membrane potential and intracellular activities of H^+ , Na^+ , or Cl^- . The results indicate that there is a pathway for HCO_3^- transport that is confined to the basolateral membrane. Furthermore, this basolateral HCO_3^- transport appears to be linked to Na^+ . This linkage can be accounted for by an electrogenic Na/ HCO_3^- transporter which carries Na^+ , HCO_3^- , and net negative charge in the same direction.

We propose that proximal-tubule acid secretion is a byproduct of intracellular pH (pH_i) regulation by the proximal tubule cells: basolateral HCO_3^- efflux lowers pH_i and thereby stimulates both luminal and basolateral Na-H exchange. Net transcellular acid secretion proceeds to the extent that H^+ extrusion occurs across the luminal rather than the basolateral membrane.

Portions of this work have been reported in preliminary form (Boron and Boulpaep, 1981a, b, 1982).

METHODS

General

We used isolated, perfused proximal tubules of the tiger salamander *Ambystoma tigrinum*. The details are presented in the preceding paper (Boron and Boulpaep, 1983).

Solutions

The compositions of the Ringer's solutions are given in Table I. Note that the numbering of solutions 1-8 is consistent with the numbering pattern used in the previous paper (Boron and Boulpaep, 1983). Solution 8 was used only for the dissection of tubules. For solution 11, [Ca] was increased threefold to compensate for Ca, which may have been chelated by the substituting anions. Solution 14 (low-substrate/HCO₃⁻), in which lactate and amino acids were deleted, was used for basolateral solutions in experiments in which SITS was used. Additional solutions,

TABLE I*

Component	1 Standard HEPES	3 pH 6.8 HEPES	4 0-Na HEPES	7 Standard HCO ₃ ⁻	8 PVP HCO ₃ ⁻	9 pH 6.8 HCO ₃ ⁻	10 0-Na HCO ₃ ⁻	11 0-Cl HCO ₃ ⁻	12 0-Cl (SO ₄ ²⁻) HCO ₃ ⁻	13 0-Na 0-Cl, HCO ₃ ⁻	14 Low-sub- strate HCO ₃ ⁻
Na ⁺	97.65	93.5	0.05	100.95	100.95	100.8	0.05	96.75	100.95	0.05	100.9
M ⁺	0	0	97.1	0	0	0	100.4	0	0	95.0	0
K ⁺	2.5	2.5	2.5	2.5	2.5	2.5	2.5	2.5	2.5	2.5	2.5
Mg ⁺⁺	1.0	1.0	1.0	1.0	1.0	1.0	1.0	1.0	1.0	1.0	1.0
Ca ⁺⁺	1.8	1.8	1.8	1.8	1.8	1.8	1.8	5.4	0.6	5.4	1.8
Lys ⁺	0.2	0.2	0.2	0.2	0.2	0.2	0.2	0.2	0.2	0.2	0.2
meq (+):	105.95	101.8	105.45	109.25	109.25	109.1	108.75	112.25	106.85	110.55	109.0
Cl ⁻	94.7	94.7	94.7	94.7	94.7	102.7	94.2	0.2	0.2	0.2	98.1
X ⁻	0	0	0	0	0	0	0	97.5	0	95.8	0
SO ₄ ²⁻	0	0	0	0	0	0	0	0	47.25	0	0
HCO ₃ ⁻	0	0	0	10.0	10.0	2.0	10.0	10.0	10.0	10.0	10.0
H ₂ PO ₄ ⁻	0.1	0.25	0.1	0.1	0.1	0.25	0.1	0.1	0.1	0.1	0.1
HPO ₄ ²⁻	0.4	0.25	0.4	0.4	0.4	0.25	0.4	0.4	0.4	0.4	0.4
Lactate ⁻	3.6	3.6	3.6	3.6	3.6	3.6	3.6	3.6	1.2	3.6	0
Glu ⁻	0.05	0.05	0.05	0.05	0.05	0.05	0.05	0.05	0.05	0.05	0
HEPES ⁻	6.7	2.7	6.7	0	0	0	0	0	0	0	0
meq (-):	105.95	101.8	105.45	109.25	109.25	109.1	108.75	112.25	106.85	110.55	109.0
Glucose	2.2	2.2	2.2	2.2	2.2	2.2	2.2	2.2	2.2	2.2	2.2
Gln	0.5	0.5	0.5	0.5	0.5	0.5	0.5	0.5	0.5	0.5	0
Ala	0.5	0.5	0.5	0.5	0.5	0.5	0.5	0.5	0.5	0.5	0
HEPES	6.7	10.7	6.7	0	0	0	0	0	0	0	0
Sucrose	0	0	9.0	0	0	0	9.0	0	50.85	9.0	0
PVP (g/l)	0	0	0	0	15	0	0	0	0	0	0
pH	7.5	6.8	7.5	7.5	7.5	6.8	7.5	7.5	7.5	7.5	7.5
CO ₂ (%)	0	0	0	1.5	1.5	1.5	1.5	1.5	1.5	1.5	1.5
O ₂ (%)	100	100	100	98.5	98.5	98.5	98.5	98.5	98.5	98.5	98.5

* Composition given in millimolar unless otherwise noted. M⁺ is a monovalent cation: either *bis*-(2-hydroxyethyl) dimethylammonium (BDA⁺), tetramethylammonium (TMA⁺), or *N*-methyl-D-glucammonium (NMDG⁺). For solutions 10 and 13, that portion of M⁺ accompanying HCO₃⁻ was always 10 mM NMDG⁺. X⁻ is a monovalent anion, either cyclamate or glucuronate. PVP is polyvinyl pyrrolidone (average molecular weight, 40,000).

not listed in Table I were also used. For example, a "0-Na/low-substrate" HCO₃⁻ Ringer was obtained by combining the recipes for solutions 10 and 14. 4-acetamido-4'-isothiocyanostilbene-2, 2'-disulfonate (SITS) was obtained from International Chemical and Nuclear (Cleveland, OH); 4,4'-dinitrostilbene-2,2'-disulfonate (DNDS) was purchased from International Chemical and Nuclear (Plainview, NY); HEPES, *N*-methyl-D-glucammonium (NMDG), tetramethylammonium-Cl, and the glucuronate salts were obtained from Sigma Chemical Co. (St. Louis, MO); and *bis*-(2-hydroxy ethyl) dimethylammonium (BDA-Cl) was purchased from Eastman Organic Chemicals (Rochester, NY). The amiloride was a gift of Merck Sharp & Dohme Research Laboratories (West Point, PA).

All solutions were delivered to pipettes or chamber by gravity through CO₂-impermeable Saran tubing (Clarkson Equipment and Controls, Detroit, MI).

Electrodes and Electronics

The Na-sensitive and pH-sensitive microelectrodes were of the recessed-tip design of Thomas (1970, 1974). The Cl-sensitive microelectrodes were of the liquid-ion exchanger type and used the Corning resin (477315; Dow Corning Corp., Midland, MI). The details concerning the construction and use of these electrodes are given in the previous paper (Boron and Boulpaep, 1983).

Curve-fitting Procedure

Rate constants of exponential pH_i recoveries were obtained by using an iterative, least-squares curve-fitting procedure to fit the data to an equation of the form $\text{pH}_i = A - B \exp(-kt)$, where k is the rate constant, and t is the time. Details are given in the previous paper (Boron and Boulpaep, 1983).

All mean values are given \pm standard error.

RESULTS

In the preceding paper (Boron and Boulpaep, 1983), we examined Na-H exchange in renal proximal tubule cells. To avoid the contribution that the flux of HCO₃⁻ (or an equivalent species) might have made to the pH_i transients, we purposely performed the preceding experiments in nominally HCO₃⁻-free solutions. The present study is devoted to an examination of basolateral HCO₃⁻ transport. Thus, the reference solution for most of these experiments was standard HCO₃⁻ Ringer (solution 7). As noted in Table II of the preceding paper, when HEPES Ringer (solution 1) is replaced by standard HCO₃⁻ Ringer, the steady state pH_i falls, and the steady state basolateral membrane potential (V_1) becomes more positive. This transition is illustrated in Fig. 1A. The application of HCO₃⁻ Ringer causes an abrupt decrease of pH_i, because of the influx of CO₂, its hydration to H₂CO₃, and the subsequent dissociation to H⁺ plus HCO₃⁻. This represents an acute intracellular acid load. In the previous paper (Boron and Boulpaep, 1983), however, we showed that a similar degree of intracellular acid loading in pH 7.5 HEPES Ringer would accelerate Na-H exchange and thereby restore pH_i to its initial level. Here, instead, with the tubule bathed in pH 7.5 HCO₃⁻ Ringer, the fall in pH_i is sustained. This failure of pH_i to recover indicates that some HCO₃⁻- or CO₂-dependent process continually loads the cell with acid as rapidly as the aforementioned Na-H exchangers can extrude the acid. Our evidence (discussed below) indicates that this process is the basolateral efflux of HCO₃⁻ and/or a related species.

The application of HCO₃⁻ Ringer also produces changes in V_1 , two patterns of which were observed. In most cases there was a monotonic and sustained basolateral depolarization (Fig. 1A); in others, this depolarization was preceded by a small, rapid hyperpolarization (see Fig. 1A, inset). The hyperpolarization is probably due to the instantaneous establishment of a highly negative diffusion potential for HCO₃⁻ or an equivalent species. As CO₂ enters the cell and generates intracellular HCO₃⁻, this diffusion potential relaxes to a value more positive than V_1 . Inasmuch as CO₂ diffusion is rapid as compared

with solution mixing in the chamber and the response time of our recording equipment, it is not surprising that the initial hyperpolarizing transient was often missed. The net, steady state basolateral depolarization is thus the combined result of the introduction of an HCO_3^- diffusion potential together with possible changes in other pH_i -sensitive ionic conductances.

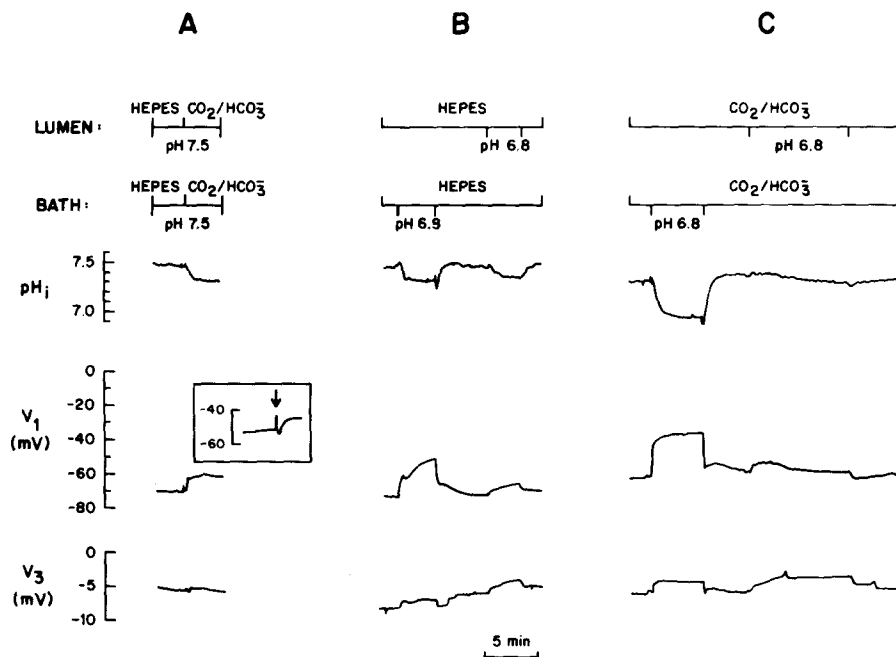


FIGURE 1. Effect of CO_2 -containing Ringer and of low extracellular pH. A. Transition from HCO_3^- -free to HCO_3^- -containing Ringer. V_1 refers to basolateral membrane potential, and V_3 to transepithelial potential difference, both referenced to the bath. In the first portion of the experiment, the tubule was exposed (lumen and bath) to a nominally HCO_3^- -free Ringer buffered with HEPES to pH 7.5 (solution 1). At the indicated time, the luminal and basolateral solutions were replaced with Ringer of the same pH, but buffered with 10 mM HCO_3^- / 1.5% CO_2 in O_2 (solution 7). This is one of 10 similar experiments, each on a separate tubule. B. Basolateral or luminal acidification in the absence of HCO_3^- . During the indicated intervals, the pH of either the basolateral or luminal solutions was reduced from 7.5 to 6.8 (solutions 1 to 3). A total of four such experiments were performed on two tubules. C. Basolateral or luminal acidification in the presence of HCO_3^- . During the indicated intervals, the pH of either the basolateral or luminal solution was reduced from 7.6 to 6.8 by reducing $[\text{HCO}_3^-]$ from 10 to 2 mM at a constant CO_2 of 1.5% (solutions 7 to 9). All experiments, except for the one in the inset, were performed on the same tubule. A total of 41 such experiments was performed on 15 different tubules.

At least three phenomena contribute to the pH_i changes that accompany the replacement of HEPES buffer with a HCO_3^- buffer: (a) the influx of CO_2 , (b) first the influx and then the efflux of HCO_3^- , and (c) the regulatory

response of the Na-H exchangers. Because of the complexity of these events, simultaneously changing $p\text{CO}_2$ and $[\text{HCO}_3^-]$ is not a useful tool for studying basolateral HCO_3^- transport. Therefore, in our first series of experiments (see *Basolateral HCO_3^- Effect* below), we opted for a protocol in which we replaced one variable (i.e., $p\text{CO}_2$) with another (i.e., pH): we altered extracellular pH (pH_o) and $[\text{HCO}_3^-]$ at constant $p\text{CO}_2$. As will be seen, this approach greatly simplifies the interpretation of pH_i transients.

Hypothesis

In the first series of experiments, we simultaneously reduced basolateral pH (pH_b) and basolateral $[\text{HCO}_3^-]$ ($[\text{HCO}_3^-]_b$) at constant $p\text{CO}_2$ while monitoring concomitant changes in pH_i , intracellular Cl^- activity (a_i^{Cl}), intracellular Na^+ activity (a_i^{Na}), V_1 , and transepithelial voltage (V_3). The following hypothesis emerged from these experiments. We propose that a SITS-sensitive carrier in the basolateral membrane transports HCO_3^- (or an equivalent species), Na^+ , and negative charge out of the cell when $[\text{HCO}_3^-]_b$ is reduced. This electrogenic Na/ HCO_3^- transporter would mediate the opposite movements when $[\text{HCO}_3^-]_b$ is returned to its initial value. For achieving such a net movement of negative charge, the ratio of HCO_3^- to Na^+ fluxes would have to exceed 1; the simplest stoichiometry is two HCO_3^- moving together with one Na^+ . This model suggested a second series of experiments in which the effects of altering $[\text{Na}^+]_b$ were examined. The predictions of the hypothesis for both series of experiments are given in Table II. Clearly, these predictions are only qualitative. Other transport systems could modify the magnitude or direction of the effects.

The remainder of the Results is divided into two parts. The first part tests predictions *a-d*, as well as the sensitivity to SITS and dependence on Cl^- . The second part tests predictions *e, g*, and *h*, as well as the SITS sensitivity and Cl^- dependence. Prediction *f* has been verified in another study (Sackin et al., 1981). Moreover, a portion of effect *f* is inhibited by SITS (Sackin, Boron, and Boulpaep, unpublished data). A prediction not included in Table II concerns the effect of altering V_1 on pH_i , a_i^{Na} , and a_i^{Cl} . However, in a leaky epithelium it is impossible to clamp the basolateral membrane independently of the luminal membrane, thus making it difficult to interpret the results. Hence this prediction has not been examined in this paper.

Basolateral HCO_3^- Effect

GENERAL DESCRIPTION Figs. 1B and C compare the effects of acidifying the luminal or basolateral solutions in HCO_3^- -free Ringer with those of similar acidifications in HCO_3^- -containing Ringer. With the tubule bathed in nominally HCO_3^- -free Ringer (solution 1), lowering either pH_b or pH_i to 6.8 (solution 3) has only a modest effect on pH_i , producing decreases of ~ 0.15 and ~ 0.10 , respectively (Fig. 1B). When either pH_b or pH_i is restored to 7.5, pH_i recovers (Fig. 1B). With the tubule bathed in HCO_3^- -containing Ringer (Fig. 1C), lowering pH_b to 6.8 (i.e., lowering $[\text{HCO}_3^-]_b$ to 2 mM; solution 9) has a much larger effect than in HCO_3^- -free Ringer, reducing pH_i by ~ 0.40 .

When $[\text{HCO}_3^-]_b$ and pH_b are returned to their initial values, pH_i recovers along an exponential time course (Fig. 1C). In 25 experiments on 11 tubules, the mean rate constant was $1.73 \pm 0.09 \text{ min}^{-1}$. Reducing luminal pH and $[\text{HCO}_3^-]$ produces only a small, slow acidification. Four aspects of the experiment of Figs. 1B and C are of particular interest.

(a) *Presence of basolateral HCO_3^- transport.* Basolateral acidification leads to a larger fall of pH_i in a HCO_3^- -containing than in a HCO_3^- -free medium (Figs. 1B and C). In both cases, the fall of pH_i is probably the result of one or more of the following four events: (i) H^+ permeability, which probably makes a rather small contribution because of the low concentration of H^+ ; (ii) HCO_3^- permeability, which in theory could produce a fall in pH_i ; (iii) Na/HCO_3 transport, which would also produce a decrease in pH_i ; (iv) inhibition of $\text{Na}-\text{H}$ exchange by the reduction of pH_b ; however, the eventual decline of pH_i would secondarily stimulate luminal $\text{Na}-\text{H}$ exchange; (v) HEPES permeability, particularly that of the neutral weak acid, whose concentration rises at low pH. The balance among the aforementioned five events will determine

TABLE II
PREDICTIONS OF HYPOTHESIS*

	Basolateral HCO_3^- effect		Basolateral Na^+ effect		
	$\downarrow [\text{HCO}_3^-]_b$	$\uparrow [\text{HCO}_3^-]_b$	$\downarrow [\text{Na}^+]_b$	$\uparrow [\text{Na}^+]_b$	
(a) pH_i	\downarrow	\uparrow	(e) pH_i	\downarrow	\uparrow
(b) a_i^{Na}	\downarrow	\uparrow	(f) a_i^{Na}	\downarrow	\uparrow
(c) ΔV_1	+	-	(g) ΔV_1	+	-
(d) a_i^{Cl}	0	0	(h) a_i^{Cl}	0	0

All the above changes are (i) blocked by SITS and (j) independent of Cl^- .

* \uparrow = increase, \downarrow = decrease, 0 = no change, + = depolarization, - = hyperpolarization.

the new steady state pH_i . The much larger fall of pH_i in pH 6.8 HCO_3^- Ringer indicates that either basolateral permeability to HCO_3^- or the Na/HCO_3 transport rate must be high.

The recovery of pH_i , when $[\text{HCO}_3^-]_b$ and pH_b are returned to their initial values, is the result of the interaction of the first four of the aforementioned mechanisms. (i) The passive flux of H^+ cannot contribute to this rise of pH_i , since the electrochemical gradients still favor H^+ influx across both luminal and basolateral membranes. (ii) The rise in pH_i cannot be accounted for by a passive influx of HCO_3^- per se, since the basolateral electrochemical gradient favors HCO_3^- efflux. (iii) However, HCO_3^- (or a related species) may be carried into the cell by the hypothesized Na/HCO_3 transporter. (iv) The pH_i recovery could in part be the result of luminal and basolateral $\text{Na}-\text{H}$ exchange. The contribution of $\text{Na}-\text{H}$ exchange will be examined in subsection *d* below.

(b) *Absence of luminal HCO_3^- transport.* Luminal acidification has very little effect on pH_i when the cells are bathed in HCO_3^- Ringer, even though a similar maneuver in HCO_3^- -free (HEPES) Ringer produces a small but

significant decline in pH_i (Figs. 1B and C). The much smaller and slower fall of pH_i that accompanies the reduction of luminal pH, as opposed to basolateral pH, indicates that the net flux of H^+ and/or HCO_3^- across the luminal membrane is much smaller than across the basolateral membrane. The small, slow fall of pH_i that occurs with luminal acidification probably reflects an inhibition of luminal Na-H exchange in the face of continued basolateral HCO_3^- efflux. The much larger fall of pH_i in 6.8 HEPES Ringer is thus probably due to the permeation by one of the members of the HEPES conjugate pair. We conclude that there is HCO_3^- transport in these cells and that it is limited to the basolateral membrane.

(c) *Electrogenic nature of basolateral HCO_3^- transport.* As shown in Figs. 1B and C, extracellular acidifications produce characteristic changes in V_1 , which are larger for basolateral than for luminal acidifications. Generally, these V_1 changes have a triphasic time course. In nominally HCO_3^- -free experiments, reducing pH_b produces (i) an abrupt depolarization of ~ 10 mV, often followed by (ii) a partial recovery, and finally followed by (iii) an additional slow, sustained, depolarization of ~ 2 mV and, exceptionally (as in Fig. 1B), up to 10 mV. Phase *i* could be caused by changes in pH_b -sensitive conductances such as K^+ (Steels and Boulpaep, 1976), and changes in the diffusion potentials of charged buffer species, such as the HEPES anion or residual HCO_3^- . Phase *ii* may be due to a secondary fall in the intracellular concentrations of a buffer anion. Phase *iii* could be due to any determinant of V_1 (e.g., an ion activity, an ion conductance, or an electrogenic transport system), which slowly responds to changes in pH_i .

For experiments in HCO_3^- Ringer, basolateral acidification (i.e., reduced $[\text{HCO}_3^-]_b$) generally produces a similar triphasic time course of V_1 , though the initial depolarization (phase *i*) is generally much larger, 25–30 mV. The partial recovery of V_1 (phase *ii*) was present in about half the cases (see Figs. 2 and 5) and amounted to 2–4 mV. The slow, sustained depolarization (phase *iii*), also observed in about half the cases, amounts to only 2–5 mV. These three phases of V_1 in the HCO_3^- Ringer would, at least in part, have the same origin as the changes in the HCO_3^- -free experiments, except for lack of HEPES contribution, a greater contribution by HCO_3^- , and a greater contribution from pH_i -sensitive determinants of V_1 . These explanations, however, cannot account quantitatively for the observed initial depolarizations (phase *i*) of 30 mV on the basis of either alterations in single-ion conductances or single-ion diffusion potentials. The H^+ conductance is unlikely to contribute significantly to V_1 . Since no chemical potential changes occur for Na^+ , K^+ , or Cl^- , these ions could only contribute to the depolarization if their permeabilities were very pH_b sensitive. Although such permeability changes could theoretically account for the initial depolarization in HCO_3^- -free Ringer, they cannot explain the threefold-larger depolarization in HCO_3^- -containing Ringer. This difference is due to the presence of HCO_3^- , although not to the diffusion potential of the bicarbonate ion.¹ Although other ions (e.g., phosphate,

¹ Reducing pH_b from 7.5 to 6.8 in HCO_3^- Ringer (Fig. 1C) instantaneously shifts the HCO_3^- equilibrium potential ($E_{\text{HCO}_3^-}$) from -12 to $+12$ mV, the proper direction for explaining a basolateral depolarization. To determine whether the magnitude of the $E_{\text{HCO}_3^-}$ shift is sufficient

NaCO_3^- , or organic weak acids and bases) undergo large fractional changes in concentration during alterations in pH_b , their concentrations are too low to influence V_1 in the absence of extraordinarily high permeabilities. We conclude that a large portion of the initial depolarization is caused by the electrogenic Na/HCO_3 transporter, which must carry net positive current into the cell when $[\text{HCO}_3^-]_b$ is lowered.

When pH_b is returned to 7.5 in HCO_3^- Ringer (Fig. 1C) there is a triphasic shift in V_1 that is a mirror image of the initial one: (i) an abrupt hyperpolarization, followed by (ii) a slight recovery of 2–4 mV, followed by (iii) a further hyperpolarization of ~5 mV. The same sort of analysis applied above to the initial depolarization can now be applied to the initial hyperpolarization. We conclude that a large portion of the initial hyperpolarization is caused by the Na/HCO_3 transporter, which must carry net positive current out of the cell when $[\text{HCO}_3^-]_b$ is raised.

Although basolateral depolarizations also occur during luminal acidification, in HCO_3^- -free or HCO_3^- -containing Ringer, these are rather small (e.g., ~5 mV). They may be the result of changes in external ion composition and/or pH_i -sensitive conductances at either the luminal membrane or shunt, or could be due to changes at the basolateral membrane, secondary to changes of intracellular composition. As to the changes in the transepithelial potential difference (V_3), these are of the same sign as those in V_1 , though much smaller, and may reflect changes at the basolateral membrane, as expected for a leaky epithelium.

(d) *Contribution of Na-H exchange to pH_i changes.* Although the above pH_i and V_1 changes, taken together, can only be accounted for by the hypothesized Na/HCO_3 transporter, the pH_i changes should also be influenced by luminal and basolateral Na-H exchange. The experiment of Fig. 2 was performed to examine the contribution of Na-H exchange to the pH_i recovery that follows restoration of $[\text{HCO}_3^-]_b$ and pH_b to normal. The tubule is exposed to HCO_3^- Ringer throughout. During six separate intervals, pH_b and $[\text{HCO}_3^-]_b$ are simultaneously lowered (solution 9) and then restored. During the first two restorations of normal pH_b and $[\text{HCO}_3^-]_b$, the recoveries of pH_i are quite rapid (rate constants, 1.94 and 2.70 min^{-1}). During the third interval of basolateral acidification, after pH_i had fallen to a new steady level, 2 mM amiloride is applied to the bath and lumen. This level of amiloride blocks ~75% of Na-H exchange in these cells (Boron and Boulpaep, 1983). The application of amiloride causes a slight rise in pH_i , which may be due to amiloride's acting as a weak base. When pH_b is subsequently returned to 7.5, pH_i recovers at a lower rate (1.30 min^{-1}) than in the two previous controls and in the succeeding

to account for the observed depolarization, we calculated a V_1 from the equation of Goldman (1943) and Hodgkin and Katz (1949). In pH 7.5 Ringer, $[\text{K}^+]_b = 2.5$, $[\text{K}^+]_i \cong 100$, $[\text{HCO}_3^-]_b = 10$, and $[\text{HCO}_3^-]_i = 6.3$ mM (calculated on the basis of $\text{pH}_i = 7.3$). Assuming that K^+ and HCO_3^- are the sole permeant ions and, moreover, that P_{HCO_3} is even as large as P_{K} , the Goldman equation predicts a V_1 of -64 mV, not far from the mean control value of -56 mV (Boron and Boulpaep, 1983). When $[\text{HCO}_3^-]_b$ is now suddenly reduced to 2 mM, the predicted V_1 changes by only 2 mV to -62 mV. This is a small fraction of the observed, initial depolarization. Thus, unless the reduction of pH_b simultaneously produces an extraordinary increase in P_{HCO_3} , the shift of E_{HCO_3} could not account for the large shift of V_1 .

one. During the fifth basolateral acidification, the amiloride test is repeated, and the pH_i recovery is once again slower than in the bracketing controls (0.94 min^{-1} vs. 2.00 and 1.77 min^{-1}). We conclude that about half the pH_i recovery rate triggered by returning pH_b to 7.5 is due to an amiloride-sensitive Na-H exchange. The balance presumably represents the basolateral uptake of HCO_3^- (or an equivalent species) mediated by the hypothetical Na/ HCO_3^- transporter.

INHIBITION BY SITS The results of the previous section suggest that the movement of HCO_3^- (or of a related species) may occur via a Na/ HCO_3^-

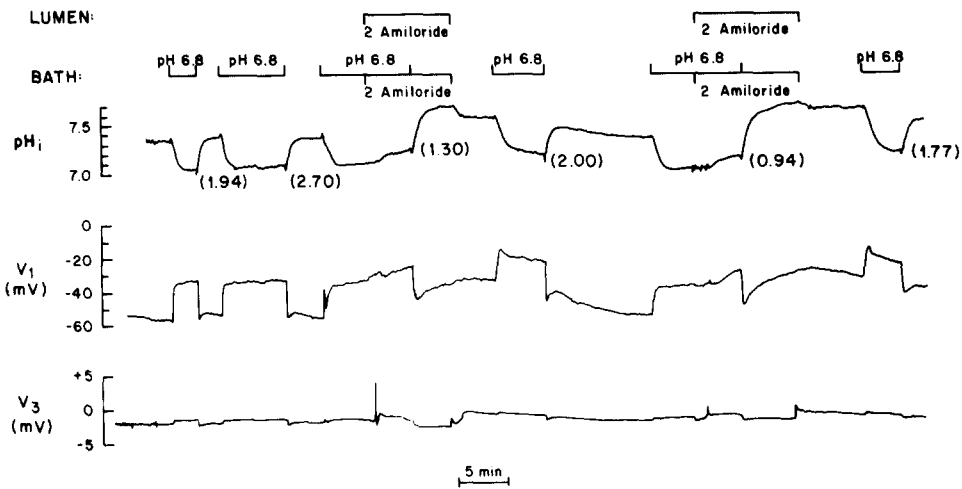


FIGURE 2. Effect of amiloride on pH_i recovery from basolateral acidification. V_1 and V_3 represent basolateral membrane potential and transepithelial potential, respectively. pH_b was lowered from 7.5 to 6.8 six times by reducing $[\text{HCO}_3^-]_b$ from 10 to 2 mM at constant CO_2 tension (solutions 7 to 9). As pH_b was returned to normal, pH_i recovered along an exponential time course; the rate constants (units: min^{-1}) are given in parentheses. 2 mM amiloride was present in bath and lumen during the third and fifth pH_i recoveries. In a separate experiment, amiloride was shown to similarly inhibit the pH_i recovery produced by returning Na^+ to the bath (experiment of Fig. 7).

transporter. Inasmuch as SITS is known to block a variety of anion transporters, we tested the effect of adding SITS (0.5 mM) to the basolateral solution. Fig. 3 illustrates an experiment in which $[\text{HCO}_3^-]_b$ and pH_b were lowered three times. In the first case (i.e., the control condition) pH_i , basolateral membrane potential, and the transepithelial potential difference change in the usual way. The subsequent application of SITS, though not shown in the figure, slightly increases pH_i and hyperpolarizes the basolateral membrane. After a 10-min pretreatment with SITS, the pH_i , V_1 , and V_3 changes elicited by reduction of $[\text{HCO}_3^-]_b$ and pH_b are greatly attenuated. In the presence of SITS the changes in pH_i and the initial changes in V_1 closely resemble those described above in the absence of HCO_3^- (see Fig. 1B). These results are

consistent with inhibition by SITS of the hypothesized Na/HCO₃ transporter. The level of sustained basolateral depolarization (phase *iii*) is also reduced by SITS. This may have two explanations. In the first place, the plateau value of V_1 may be pH_i dependent and thus mirror the plateau value of pH_i. Second, the magnitude of the sustained depolarization may normally be determined by the continued transport of charge by the Na/HCO₃ transporter, and thus may be reduced when the transporter is inhibited by SITS.

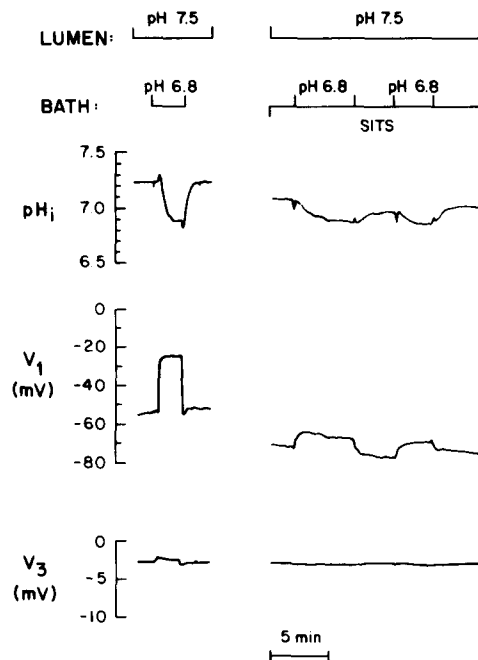


FIGURE 3. Effect of SITS on basolateral-acidification-induced changes. V_1 and V_3 represent basolateral membrane potential and transepithelial potential, respectively. During the indicated three intervals, pH_b was lowered from 7.5 to 6.8 by reducing [HCO₃]_b from 10 to 2 mM at constant pCO₂ (solutions 7 to 9). The rate constants for the pH_i recovery from the basolateral acidifications (units: min⁻¹) are given in parentheses. Beginning 5 min before, and continuing throughout the final two pH 6.8 pulses, the tubule was exposed to 0.5 mM SITS in the basolateral solution. This is one of six such experiments on three separate tubules.

LACK OF CL⁻ INVOLVEMENT Although the hypothesized, electrogenic Na/HCO₃ cotransporter seems necessary to account for the data of the previous two sections, we have not yet ruled out that a portion of the HCO₃⁻ movement is mediated by an electroneutral Cl⁻-HCO₃⁻ exchanger or by a Na/HCO₃-Cl⁻/H exchanger. The possibility of a linkage of Cl⁻ to HCO₃⁻ is raised by the observation that the steady state a_i^{Cl} is higher in the nominal absence than in the presence of HCO₃⁻ (Boron and Boulpaep, 1983; Guggino et al., 1982).

(a) pH_i changes. In the experiment of Fig. 4, the effect of basolateral acidification is tested in the absence of Cl^- (HCO_3^- present throughout). The tubule is first subjected to a basolateral acidification in the presence of Cl^- , which produces the usual changes in pH_i and V_1 . Removal of Cl^- from the bath and lumen (solution 11; Cl^- replaced by cyclamate) causes pH_i to slowly decrease by ~ 0.2 . If $HCO_3^-Cl^-$ or $Na/HCO_3^-Cl^-/H$ exchange were a major

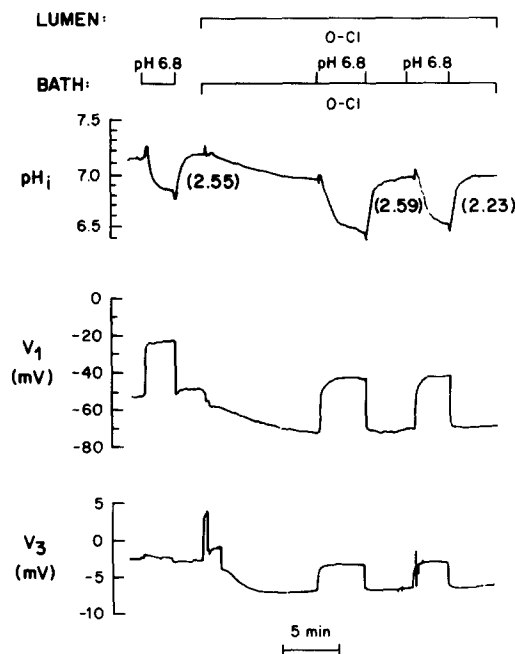


FIGURE 4. Effect of Cl^- removal on basolateral-acidification-induced changes. V_1 and V_3 represent basolateral membrane potential and transepithelial potential, respectively. During the indicated intervals, pH_b was reduced from 7.5 to 6.8 by lowering $[HCO_3^-]_b$ from 10 to 2 mM at constant CO_2 tension. Before and during the second and third acidifications, Cl^- was replaced, bath and lumen, with cyclamate (solution 11). The rate constants for the pH_i recoveries (units: min^{-1}) are given in parentheses. Although the phase *ii* hyperpolarization is not evident in the absence of Cl^- in this experiment, it has been observed in other experiments (not shown). A total of eight similar experiments was performed on four separate tubules.

pathway for basolateral HCO_3^- flux, Cl^- removal should instead have raised pH_i . After 10 min in Cl^- -free Ringer (a period sufficient to remove most intracellular Cl^- ; see Fig. 5), reducing pH_b and $[HCO_3^-]_b$ has about the same effect on pH_i as under control conditions. Returning pH_b and $[HCO_3^-]_b$ to normal causes a pH_i recovery which is about as rapid ($k = 2.59$ and $2.23 min^{-1}$) as in the presence of Cl^- ($k = 2.55 min^{-1}$). In six paired experiments on three tubules, the mean rate constant in Cl^- -containing solutions was $2.07 \pm 0.26 min^{-1}$, not significantly different from $1.91 \pm 0.28 min^{-1}$, the value in

Cl^- -free solutions (paired *t* test, $P = 0.33$). The experiment of Fig. 4 has been repeated while replacing Cl^- with either glucuronate (solution 11) or SO_4^- (solution 12), with similar results. These data indicate that most of the movement of HCO_3^- (or an equivalent species) and the movement of charge across the basolateral membrane are not dependent on Cl^- . We cannot, however, rule out a small component of HCO_3^- -Cl exchange.

(b) *Voltage changes.* The removal of Cl^- (replaced with cyclamate) causes a basolateral hyperpolarization, as observed by others (Anagnostopoulos and Planelles, 1979; Guggino et al., 1982) when Cl^- is removed in solutions of

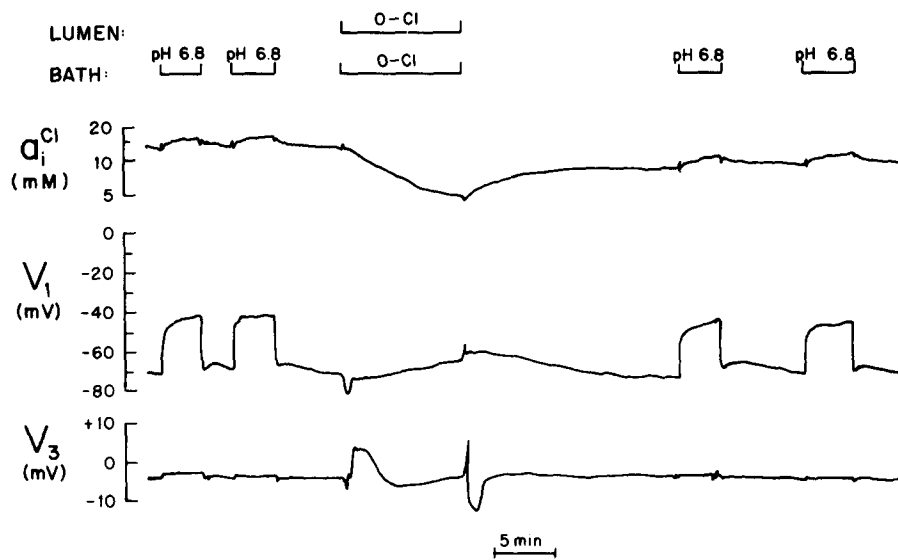


FIGURE 5. Intracellular Cl^- activity during basolateral acidification and during Cl^- removal. V_1 and V_3 represent basolateral membrane potential and transepithelial potential, respectively. pH_b was reduced from 7.5 to 6.8 four times by lowering $[\text{HCO}_3^-]_b$ from 10 to 2 mM at constant CO_2 tension (solutions 7 to 9). Between the second and third acidifications, Cl^- was replaced with glucuronate (solution 11) in both the bath and lumen to demonstrate that the Cl^- electrode could indeed detect changes in a_i^{Cl} . A total of 18 such experiments was performed on five separate tubules.

near-constant Ca^{++} activity. When Cl^- is replaced with glucuronate, as in the experiment of Fig. 5, the hyperpolarization is only transient. The magnitude of the subsequent basolateral-acidification-induced depolarization (phase *i*) is unaffected by Cl^- removal. These two results are consistent with a low basolateral Cl^- conductance.² In contrast, a high paracellular Cl^- conductance

² The sign of the V_1 change upon Cl^- removal is opposite to that expected of a membrane with a high Cl^- conductance. In addition, the magnitudes of the basolateral acidification-induced depolarizations are the same with and without Cl^- . Because the decreases in pH_i , and therefore the amount of current carried by the hypothesized Na/HCO_3 transporter, are the same in the two cases, the basolateral-membrane resistance must also have been the same with and without Cl^- . Hence, Cl^- conductance is low.

is indicated by the transepithelial hyperpolarization caused by removal of Cl^- , as previously noted (Sackin and Boulpaep, 1981*b*). The larger basolateral-acidification-induced V_3 changes seen in Cl-free as opposed to Cl-containing solutions are also consistent with a larger IR drop due to an increased paracellular resistance.

(c) a_i^{Cl} changes. As a final test for the involvement of Cl^- , we monitored changes in a_i^{Cl} during four periods in which pH_b and $[\text{HCO}_3^-]_b$ were lowered in HCO_3^- Ringer (Fig. 5). Basolateral acidification produces an abrupt 1–2 mM increase in a_i^{Cl} , followed a slower increase of another ~ 2 mM over 5 min. When pH_b and $[\text{HCO}_3^-]_b$ are returned to normal, a_i^{Cl} falls over the course of several minutes. To verify that the Cl^- microelectrode was functioning properly, we exposed the tubule, from both the bath and lumen, to a Cl-free solution (solution 11). This causes the apparent a_i^{Cl} to fall to ~ 5 mM. In seven such experiments, the minimal apparent a_i^{Cl} in Cl-free Ringer was 5.5 ± 0.7 mM; the residual Cl^- signal may represent cross-sensitivity of the Cl^- electrode to other anions. When comparing the a_i^{Cl} changes of Fig. 5 with the pH_i changes of Figs. 1–4, it is important to note that when $[\text{HCO}_3^-]_b$ and pH_b are reduced, the slow phase of the a_i^{Cl} increase has a much longer time course than the fall in pH_i . Thus, this slow phase of the a_i^{Cl} rise is probably not caused by the same mechanism responsible for the rapid fall of pH_i . It may be due to another HCO_3^- -linked transporter or to a change in pH_i -sensitive Cl^- transport. As for the rapid phase of the a_i^{Cl} increase, its magnitude is far too small to account for the observed fall in pH_i on the basis of either a one-for-one Cl- HCO_3^- exchange or a Na/ HCO_3^- -Cl/H exchange (which is equivalent to one Cl^- for two HCO_3^-).³

INVOLVEMENT OF Na^+ In the experiment of Fig. 6, we monitored a_i^{Na} while simultaneously reducing pH_b from 7.5 to 6.8 and $[\text{HCO}_3^-]_b$ from 10 to 2 mM. During both basolateral acidifications of Fig. 6A, a_i^{Na} declines with about the same course as the fall in pH_i that occurs under these conditions (see Figs. 1–4). As the basolateral acidification is maintained, a_i^{Na} gradually recovers. The initial fall of a_i^{Na} could result from either decreased Na^+ entry or increased Na^+ exit. Decreased, presumably luminal, entry of Na^+ could be caused by the depolarization of the luminal membrane, which can be inferred from the changes in V_1 and V_3 . However, we would expect this to lead to a monotonic fall of a_i^{Na} as the declining Na^+ pump rate once again comes into balance with the reduced Na^+ influx. The biphasic nature of the fall in a_i^{Na} is better explained by a sudden, transient exit of Na^+ , which is somehow linked to the reduction of either $[\text{HCO}_3^-]_b$ or pH_i . It is unlikely that a pH_i -sensitive

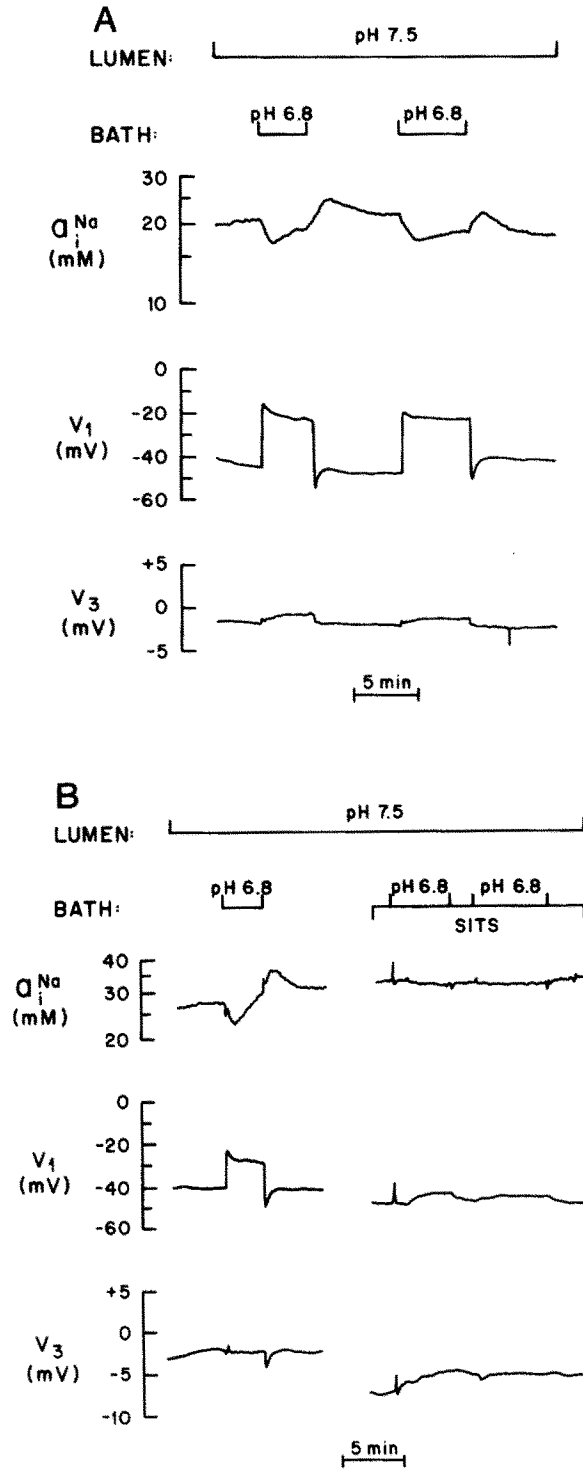
³ Taking the intrinsic intracellular buffering power (β_i) as 36 mM (Boron and Boulpaep, 1983) and the CO_2 buffering power (β_{CO_2}) as $2.3 \cdot [\text{HCO}_3^-]_i$ (see Roos and Boron, 1981) or 9 mM, the total intracellular buffering power ($\beta_T = \beta_i + \beta_{\text{CO}_2}$) comes to 45 mM. Thus, a pH_i decrease of 0.4 corresponds to the net exit of $45 \times 0.4 = 18$ mmol HCO_3^- (or an equivalent species) per liter intracellular fluid, substantially greater than the observed increment in a_i^{Cl} . Since this comparison neglects the possible contribution of other Cl^- pathways for regulating a_i^{Cl} , the slow rise in a_i^{Cl} of Fig. 5 may underestimate the Cl^- influx mediated by Cl- HCO_3^- exchange or Na/ HCO_3^- -Cl/H exchange.

Na-K pump would exhibit a biphasic response in view of the monotonic fall in pH_i . We suspect that the sudden exit of Na^+ is caused by the hypothesized Na/HCO_3^- transporter. A portion of the recovery of a_i^{Na} may be due to stimulation of luminal Na-H exchange, secondary to the fall in pH_i . Restoring pH_b to 7.5 produces an overshoot of a_i^{Na} , followed by a gradual return of a_i^{Na} to its initial value. The overshoot of a_i^{Na} is probably caused by a rapid and transient entry of Na^+ , associated with the simultaneous, basolateral entry of HCO_3^- . Subsequently, a_i^{Na} returns to its initial value as the activity of the Na-K pump overtakes the now-declining Na^+ entry. Fig. 6B illustrates the effect of SITS on these a_i^{Na} transients. During the first period of basolateral acidification, in the absence of SITS, the usual changes in a_i^{Na} , V_1 , and V_3 are observed. With the addition of SITS to the basolateral solution, however, basolateral acidification produces no change in a_i^{Na} . We do not show here an experiment in which we found that removal of Cl^- has no effect on these changes in a_i^{Na} . The fall of a_i^{Na} associated with basolateral acidification, and the blockade of this fall by SITS, suggests but does not prove that basolateral Na^+ and HCO_3^- transport are coupled.

Basolateral Na⁺ Effect

GENERAL DESCRIPTION To determine whether the hypothesized electrogenic HCO_3^- transporter is, indeed, linked to Na^+ , we performed experiments in which we removed Na^+ from the bath or the lumen, while continuously exposing the tubule to pH 7.5 HCO_3^- Ringer. In the experiment of Fig. 7A, Na^+ was absent (replaced with TMA^+) from the lumen throughout (solution 10). Subsequent removal of basolateral Na^+ causes pH_i to fall by >0.3 and produces a large, transient depolarization of the basolateral membrane. Returning Na^+ to the bath causes a rapid recovery of pH_i and a large, transient basolateral hyperpolarization, which in some cases reached -140 mV. The experiment of Fig. 7B, on a second tubule, compares the effects of removing luminal and basolateral Na^+ . Removal of luminal Na^+ causes a small, slow fall in pH_i , followed by a recovery. In addition, there is a basolateral hyperpolarization (amounting to ~ 20 mV in this case), followed by a partial recovery, as well as a gradual transepithelial depolarization.

(a) *Presence of basolateral Na/HCO₃ transport.* One would expect that removing basolateral Na^+ should lower pH_i in virtue of blocking basolateral Na-H exchange. Similarly, returning basolateral Na^+ should restore basolateral Na-H exchange and thereby return pH_i to normal. However, changes in the basolateral Na-H exchange rate are unlikely to explain fully the pH_i changes elicited by altering $[\text{Na}^+]_b$. First, the fall in pH_i caused by removing basolateral Na^+ is much more striking than that produced by removing luminal Na^+ . The evidence for Na-H exchange in HCO_3^- -free Ringer (Boron and Boulpaep, 1983) indicates that Na^+ removal should be only slightly more effective from the basolateral than from the luminal side. Second, the pH_i recoveries of Figs. 7A and B have rate constants of ~ 2.0 and $\sim 2.6 \text{ min}^{-1}$, respectively, substantially higher than expected for Na-H exchange alone, $\sim 1.0 \text{ min}^{-1}$ (Boron and Boulpaep, 1983). Therefore, these pH_i changes must be mediated in part by



another mechanism, presumably the electrogenic Na/HCO₃ transporter, in accord with prediction *e* of Table II.

(*b*) *Absence of luminal Na/HCO₃ transport.* The difference between the pH_i changes produced by basolateral vs. luminal Na⁺ removal indicate a lack of a substantial Na/HCO₃ flux across the luminal membrane. In Fig. 7B, the modest fall of pH_i caused by luminal Na⁺ removal is probably caused by blockage of luminal Na-H exchange. In addition, the accompanying basolateral hyperpolarization, which reflects luminal Na⁺ conductance in this leaky epithelium (Sackin and Boulpaep, 1981*b*), may enhance basolateral Na/HCO₃ efflux. The subsequent pH_i recovery (i.e., preceding basolateral Na⁺ removal) may be due to increased basolateral Na-H exchange secondary to the fall of a_i^{Na} , as well as to a slowing or reversal of basolateral Na/HCO₃ transport secondary to decreases of pH_i and a_i^{Na} .

(*c*) *Electrogenic nature of Na/HCO₃ transporter.* The results of Figs. 7A and B confirm prediction *g* of Table II, that removal of basolateral Na⁺ should produce an abrupt basolateral depolarization. Furthermore, as the exit of HCO₃⁻, Na⁺, and net negative charge gradually slows, the depolarization should decay. The opposite fluxes and charge movement should occur when basolateral Na⁺ is restored, thereby producing the opposite changes in V_1 .

An alternative explanation for the changes in V_1 produced by these alterations of [Na⁺]_b is that the V_1 changes reflect alterations of the electrogenic Na-K pump rate. To test this hypothesis, we performed the experiment of Fig. 8, in which Na⁺ was absent from the lumen throughout. In the first two sequences, basolateral Na⁺ is removed as usual, and the standard changes in V_1 are observed. During the third removal of Na⁺, ouabain (10⁻⁴ M) is added to the basolateral solution. When Na⁺ is finally added back to the basolateral solution, after a 20-min pretreatment with ouabain, the spiking basolateral hyperpolarization still occurs, even though the Na-K pump is presumably blocked. It is interesting to note that with the Na-K pump blocked, and therefore presumably with a higher-than-normal a_i^{Na} , the subsequent basolateral removal of Na⁺ causes a larger initial basolateral depolarization (Fig. 8, the fourth and fifth Na⁺ removals). This is expected if the Na/HCO₃ efflux is sensitive to the Na⁺ electrochemical gradient.

INHIBITION BY SITS Fig. 9 illustrates the effect of SITS on the pH_i and V_1 changes induced by the basolateral removal and reapplication of Na⁺. Note that Na⁺ is present in the lumen throughout. Under control conditions, changes in basolateral Na⁺ have the same general effects as pointed out for

FIGURE 6. (*opposite*) A. Intracellular Na⁺ activity during basolateral acidification. V_1 and V_3 represent basolateral membrane potential and transepithelial potential, respectively. Twice pH_b was lowered from 7.5 to 6.8 by lowering [HCO₃⁻] from 10 to 2 mM at constant CO₂ tension (solutions 7 to 9). A total of 18 similar experiments was performed on six separate tubules. B. Effect of SITS on Na⁺ activity changes induced by basolateral acidification. This second tubule was treated with 0.5 mM basolateral SITS for ~5 min before the second and third pH 6.8 pulses. The gap represents a period of 13 min. A total of three experiments was performed on two separate tubules.

Fig. 7, where Na^+ was absent from the lumen. With SITS present in the bath, however, removal of basolateral Na^+ does not elicit the rapid fall in pH_i normally observed or the usual changes in V_1 and V_3 . This suggests that SITS blocks the electrogenic Na/HCO_3 transporter, in agreement with prediction *i* of Table II.

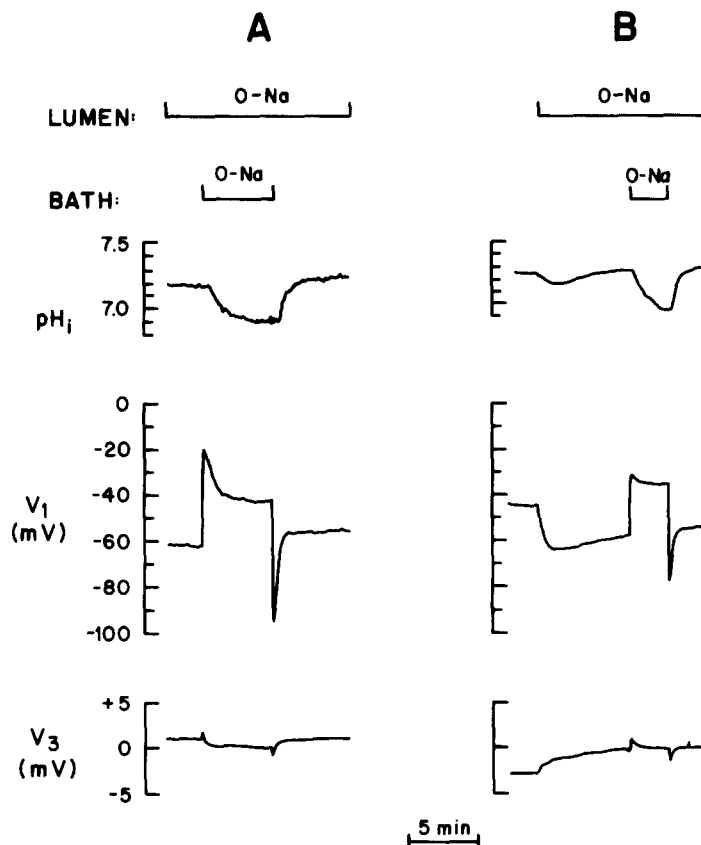


FIGURE 7. A. Effect of basolateral Na^+ removal. V_1 and V_3 represent basolateral membrane potential and transepithelial potential, respectively. Luminal Na^+ was replaced with TMA^+ (solution 10) 15 min before Na^+ was removed from the bath. Although not pronounced in this example, in many experiments the removal and readdition of basolateral Na^+ produced triphasic shifts in V_1 , much as did basolateral reduction and restoration of $[\text{HCO}_3^-]_b$. B. Comparison of luminal and basolateral Na^+ removal (second tubule). pH was 7.5 throughout. A total of 63 similar experiments was performed on 36 separate tubules.

In the absence of SITS (Fig. 9, first pulse), Na^+ removal causes a transient depolarization followed by a slower phase of depolarization (phase *iii*), in contrast to Fig. 7. The slower depolarization in Fig. 9 is due to the presence of Na^+ in the lumen and, therefore, to a higher a_i^{Na} , which sustains a higher rate of electrogenic Na/HCO_3 exit throughout the period of basolateral Na^+

removal. This is manifested by a greater phase *iii* basolateral depolarization as well as by a transepithelial depolarization. In the presence of SITS, Na^+ removal causes a transient basolateral hyperpolarization, rather than the usual depolarization. Also, the transient transepithelial depolarization is replaced by a sustained hyperpolarization. These changes may be due to Na^+ diffusion potentials across both the shunt and the basolateral membrane; these effects are of opposite sign to those induced by the electrogenic Na/HCO_3 transporter.

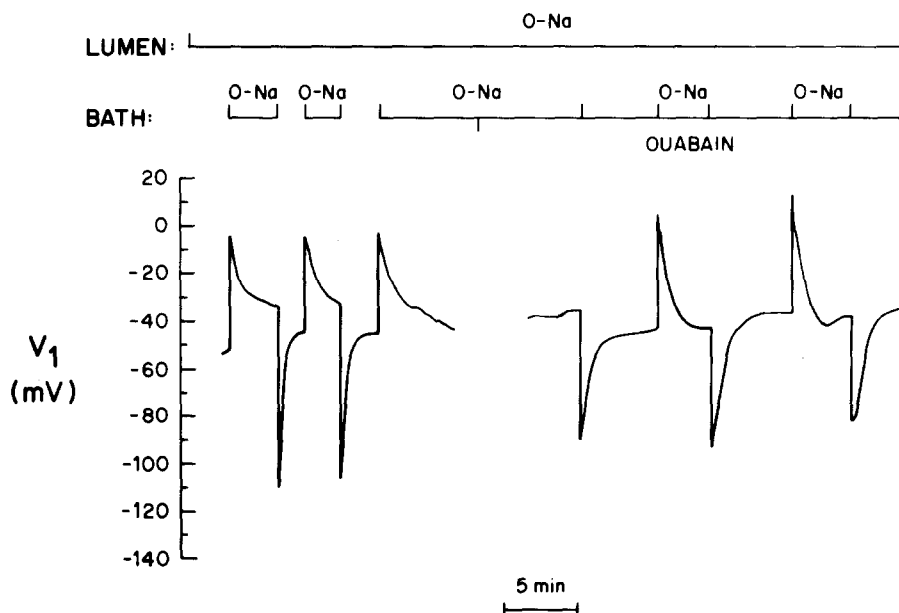


FIGURE 8. Effect of ouabain on basolateral membrane potential changes induced by changes in basolateral $[\text{Na}^+]$. V_1 and V_3 represent membrane potential and transepithelial potential, respectively. Luminal Na^+ was absent throughout (replaced with NMDG^+). The first two intervals of basolateral Na^+ removal (solutions 7 to 10) were performed in the usual way. After the third basolateral Na^+ removal, however, 10^{-4} M ouabain was added to the basolateral solution. Inasmuch as a_i^{Na} was already probably very low before the application of ouabain, the ouabain probably did not lead to any build-up of intracellular Na^+ before the third reintroduction of Na^+ . Na^+ was removed and readmitted twice more in the continued presence of ouabain. This was the only such experiment performed.

Whereas the experiment of Fig. 9 demonstrates inhibition by SITS of Na/HCO_3 exit, that of Fig. 10 is designed to determine whether SITS also inhibits the Na/HCO_3 entry. Removing Na^+ first from the lumen and then from the bath causes the usual changes in pH_i (see Fig. 7), followed by a rapid pH_i recovery (rate constant, 2.13 min^{-1}) upon restoration of basolateral Na^+ . After a second removal of basolateral Na^+ , SITS is added to the bath. Reapplication of Na^+ now elicits a pH_i recovery that is slower than in the absence of SITS

(rate constant, 1.08 min^{-1}). Table III summarizes a total of seven such experiments, and shows that the mean rate constant for pH_i recovery in the absence of SITS (k_{HCO_3}) is about twice as great as in the presence of SITS (k_{SITS}). This difference is statistically significant. The value of k_{SITS} is close to 0.96 ± 0.02 , the rate constant for basolateral Na-H exchange, which is SITS insensitive (Boron and Boulpaep, 1983). These results suggest that the pH_i

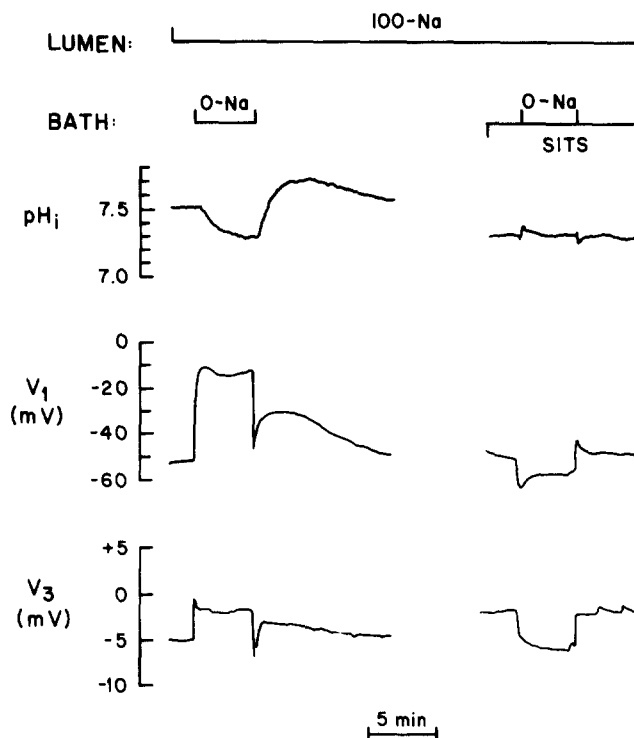


FIGURE 9. Effect of SITS on changes induced by changes in basolateral $[\text{Na}^+]$. V_1 and V_3 represent basolateral membrane potential and transepithelial potential, respectively. In the first portion of the experiment, basolateral Na^+ was removed in the usual way (replaced by BDA^+). The gap represents an interval of 38 min. Basolateral SITS (0.5 mM) was applied 33 min before the second period of Na^+ removal. pH_b and pH_i were 7.5 throughout. Note that 100 mM Na^+ was present in the lumen. A total of 15 experiments similar to the ones in this figure and Fig. 10 was performed on 14 separate tubules.

recovery in the presence of SITS is mediated by basolateral Na-H exchange alone, whereas the pH_i recovery in the absence of SITS is mediated by two parallel basolateral events, Na-H exchange and the electrogenic Na/HCO_3 influx.

When the basolateral Na^+ is finally removed, as shown in Fig. 10, in the presence of SITS, pH_i slowly falls. This is in contrast to the stability of pH_i in the experiment of Fig. 9. The discrepancy may be due to the presence of

luminal Na^+ , and thus of luminal Na-H exchange, in Fig. 9. The presence or absence of Na^+ in the lumen may also account⁴ for the discrepancies in voltage changes between Figs. 9 and 10.

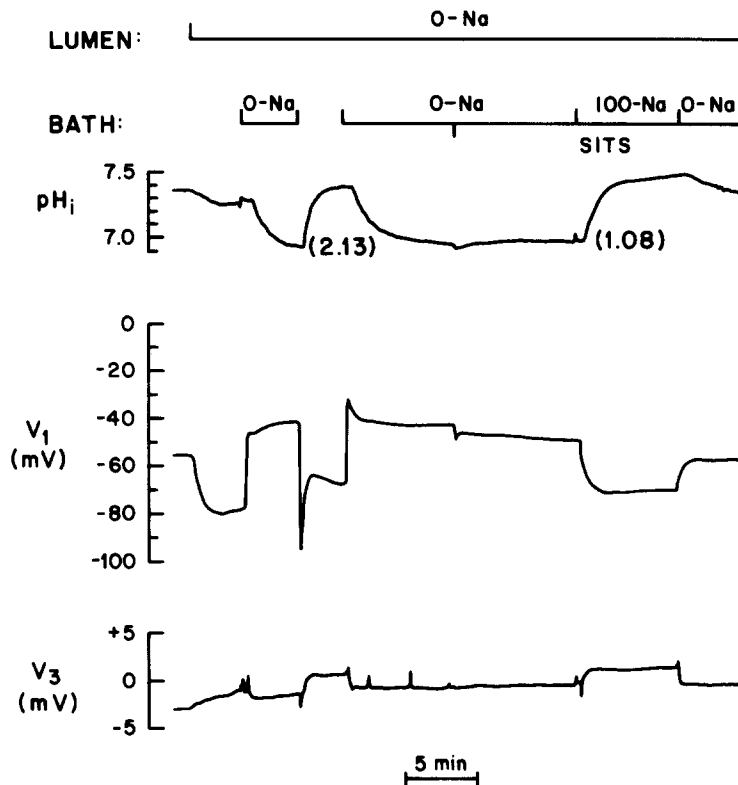


FIGURE 10. Effect of SITS on pH_i recovery accompanying restoration of 100 mM basolateral Na^+ . V_1 and V_3 represent basolateral membrane potential and transepithelial potential, respectively. Na^+ was first removed (solutions 7 to 10) from the luminal (replaced by TMA^+) and then the basolateral solution. Restoring $[\text{Na}^+]_b$ to 100 mM caused a rapid pH_i recovery (rate constant, 2.13 min^{-1}). After the second removal of basolateral Na^+ , SITS was applied. The pH_i recovery upon restoring $[\text{Na}]_b$ to 100 mM this time was much slower (rate constant, 1.08 min^{-1}). pH_b and pH_i were 7.5 throughout. A total of 15 experiments similar to the ones in this figure and Fig. 9 was performed on 14 separate tubules.

⁴ The reapplication of basolateral Na^+ in the presence of SITS causes a basolateral hyperpolarization in Fig. 10, as opposed to a smaller depolarization in Fig. 9. There are two major differences between the experiments of Fig. 9 and 10 with regard to the readmittance of basolateral Na^+ . (i) In Fig. 9 there is 100 mM Na^+ present in the lumen, whereas Na^+ is absent in Fig. 10. (ii) In Fig. 10 there is a pH_i recovery, whereas in Fig. 9 there is none. The hyperpolarization of Fig. 10 is probably related to the simultaneous recovery of pH_i , and was also observed in the terminal portion of Fig. 5 in the preceding paper (Boron and Boulpaep,

INVOLVEMENT OF HCO_3^- The electrogenic Na/HCO_3 hypothesis predicts that the basolateral $[\text{Na}^+]$ effect should depend on HCO_3^- . In the first half of Fig. 11, simultaneous removal of luminal and basolateral Na^+ in HCO_3^- -free Ringer causes pH_i to fall slowly by nearly 0.40 over a 10-min period. This decrease is probably due to abolition of Na-H exchange and/or reversal of the Na-H exchangers. Reintroduction of basolateral Na^+ causes pH_i to recover with a rate constant of 0.37 min^{-1} , probably because of basolateral Na-H exchange alone. The failure of pH_i to return to its initial value probably reflects a rather high rate of metabolic acid production in this tubule. The basolateral addition of Na^+ in HCO_3^- -free Ringer also causes a slow, sustained hyperpolarization, in contrast to the hyperpolarizing V_1 spike normally seen in HCO_3^- Ringer (Fig. 7), but similar to the sustained hyperpolarization seen with SITS in HCO_3^- Ringer (Fig. 10). The subsequent readdition of luminal

TABLE III
EFFECT OF SITS ON pH_i RECOVERY AFTER RETURNING
BASOLATERAL Na^+ *

Tubule	k_{HCO_3} min^{-1}	k_{SITS} min^{-1}	$k_{\text{HCO}_3}/k_{\text{SITS}}$
080180A	1.28	1.00	1.28
080180B	2.39	1.10	2.17
080180C	2.13	1.08	1.97
080580A	1.33	0.41	3.24
080580B	1.40	0.84	1.67
080680C	1.34	0.75	1.79
080780A	1.46	0.59	2.46
	1.62 ± 0.17	0.82 ± 0.10	2.01

* k_{HCO_3} is the control rate constant in HCO_3^- Ringer; k_{SITS} is the rate constant in HCO_3^- Ringer containing 0.5 mM SITS in the bath. One rate constant for each was measured per tubule. The mean k_{HCO_3} is significantly different from the mean k_{SITS} (paired t test; $P < 0.0004$). The mean $k_{\text{HCO}_3}/k_{\text{SITS}}$ was obtained assuming a log-normal distribution. Luminal solutions were all Na-free so that the pH_i recovery rates were minimally contaminated by luminal events.

Na^+ causes a further recovery of pH_i . The transient basolateral depolarization produced by reapplication of Na^+ to the lumen probably reflects a luminal Na^+ conductance.

In the second half of the experiment of Fig. 11, the HCO_3^- -free Ringer is replaced with standard HCO_3^- Ringer, leading to the usual sustained fall in pH_i and the depolarization of V_1 . Simultaneous removal of luminal and basolateral Na^+ now leads to a fall in pH_i , which, when compared with the sequence in HCO_3^- -free Ringer, is both more rapid (initial rate, 0.166 vs. 0.072 pH units/min) and of greater magnitude (0.50 vs. 0.40). In addition, there is a transient basolateral depolarization rather than a hyperpolarization. These

1983), where pH_i recovery was also mediated solely by basolateral Na-H exchange. The transepithelial voltage changes associated with alterations of $[\text{Na}^+]_b$ in Fig. 10 are probably due to changes in the Na^+ diffusion potential at the shunt.

differences are probably due to basolateral Na/HCO_3 efflux. When Na^+ is now readmitted to the basolateral solution, pH_i recovers more rapidly than it had in the absence of HCO_3^- (rate constant, 1.05 vs. 0.37 min^{-1}). There is also a transient basolateral hyperpolarization instead of a depolarization.

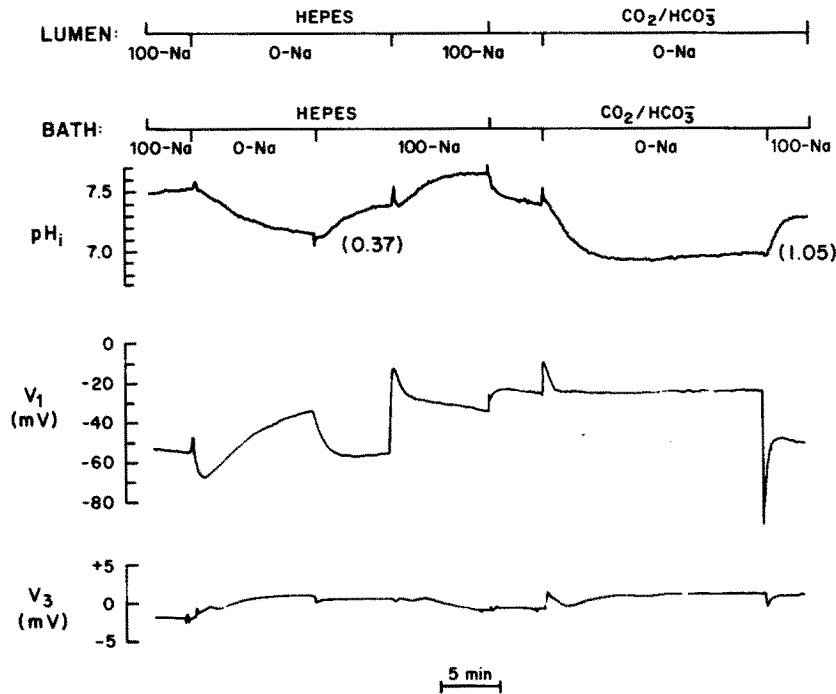


FIGURE 11. Dependence on HCO_3^- of pH_i recovery accompanying restoration of $[\text{Na}^+]_b$ to 100 mM. V_1 and V_3 represent basolateral membrane potential and transepithelial potential, respectively. In the first part of the experiment, the Ringer was nominally HCO_3^- -free HEPES (solution 1). Na^+ removal (solution 4) from both bath and lumen (replaced with TMA^+) produces a slow fall in pH_i and a transient basolateral hyperpolarization. The latter is probably due to a luminal Na^+ conductance. A hyperpolarization was also observed when luminal Na^+ was removed in the first part of Fig. 10. Returning Na^+ to the bath caused pH_i to recover slowly (rate constant, 0.37 min^{-1}). Na^+ was later returned to the lumen. The HEPES Ringer was then replaced with 1.5% $\text{CO}_2/10 \text{ mM HCO}_3^-$ Ringer at the same pH (7.50) in both the bath and lumen (solution 7), causing a fall in pH_i . After simultaneous removal of luminal and basolateral Na^+ (solution 10) and subsequent restoration of $[\text{Na}^+]_b$ to 100 mM, pH_i recovered rapidly (rate constant, 1.05 min^{-1}). A total of 17 similar experiments was performed on 10 separate tubules.

Table IV summarizes the mean rate constants for pH_i recovery in HCO_3^- -free (k_{HEPES}) vs. HCO_3^- -containing (k_{HCO_3}) Ringer. The paired difference between k_{HEPES} and k_{HCO_3} is statistically significant. When adjusted for the

difference in intracellular buffering power,⁵ the mean k_{HCO_3} is about twice as large as the mean k_{HEPES} . This is close to the $k_{\text{HCO}_3}/k_{\text{SITS}}$ ratio of Table III, 2.01, and provides further support for the hypothesis that the pH_i recovery produced by the reintroduction of basolateral Na^+ in HCO_3^- Ringer is mediated by two parallel processes, basolateral Na-H exchange and basolateral Na/HCO_3 uptake.

LACK OF Cl^- INVOLVEMENT The hypothesis of the electrogenic Na/HCO_3 transporter predicts that the changes of pH_i induced by alterations of $[\text{Na}^+]_b$ should not be affected by removal of Cl^- (Table II, prediction *j*), and should not be accompanied by changes of a_i^{Cl} (prediction *h*). These predictions were tested in two series of experiments. In the first (Fig. 12), we tested whether Cl^- is necessary for the pH_i changes that normally occur as $[\text{Na}^+]_b$ is altered. The first and third basolateral removals of Na^+ produce the same effects as pointed

TABLE IV
 HCO_3^- DEPENDENCE OF pH_i RECOVERY AFTER RETURNING
 BASOLATERAL Na^+*

Tubule	k_{HCO_3}	k_{HEPES}	Corrected $k_{\text{HCO}_3}/k_{\text{HEPES}}^5$
081380A	2.49±0.25 (4)	0.94±0.46 (2)	3.31
081480A	3.08 (1)	2.06 (1)	1.87
081480B	1.23 (2)	1.30 (1)	1.18
082080A	1.16±0.18 (5)	0.54 (1)	2.69
082180A	0.94±0.05 (4)	0.44±0.03 (4)	2.67
082180B	1.33±0.05 (2)	0.77±0.24 (2)	2.16
	1.71±0.36	1.01±0.24	2.20

* k_{HCO_3} is the rate constant in HCO_3^- Ringer; k_{HEPES} is the rate constant in HCO_3^- -free HEPES Ringer. The mean k_{HCO_3} is significantly different from the mean k_{HEPES} (paired *t* test; $P < 0.013$). The mean $k_{\text{HCO}_3}/k_{\text{HEPES}}$ was obtained assuming a log-normal distribution. The number of experiments per tubule given in parentheses. Luminal solutions were all Na-free to minimize the contribution of luminal Na-H exchange to the pH_i recoveries.

out for Fig. 7A. Readdition of basolateral Na^+ causes pH_i to recover with rate constants of 0.70 and 0.47 min^{-1} , respectively. When Cl^- was removed from both the bath and lumen, the rate constant of the pH_i recovery upon readdition of Na^+ was 0.51 min^{-1} , only slightly less than the preceding control, and actually somewhat greater than the succeeding control. Table V summarizes the results of similar experiments on a total of five tubules. The mean rate constants for pH_i recovery in the presence (k_{HCO_3}) and in the absence

⁵ The rate constant of the pH_i recovery is inversely proportional to the total intracellular buffering power (β_T). In HCO_3^- -free (HEPES) Ringer, β_T is simply the buffering power of intrinsic intracellular buffers, ~36 mM (Boron and Boulpaep, 1983). However, when the cells are bathed in 1.5% CO_2 Ringer, the presence of ~4 mM HCO_3^- in the intracellular fluid raises β_T to ~45 mM. Therefore, the ratio of k_{HEPES} to k_{HCO_3} must be corrected by the factor 45/36 = 1.25. The mean of the ratio $k_{\text{HCO}_3}/k_{\text{HEPES}}$ (corrected for the β_T discrepancy) was 2.20, assuming a log-normal distribution.

($k_{0,Cl}$) of Cl^- were not significantly different, which suggests that Cl^- does not participate in the operation of the electrogenic Na/HCO_3 transporter.

In a second series of experiments we monitored a_i^{Cl} while altering $[Na^+]_b$. In the experiment of Fig. 13, Na^+ , initially present in the lumen and bath, is removed from the basolateral solution. This causes a_i^{Cl} to rise rather rapidly over the first ~ 40 s, and then more slowly over the duration of the basolateral

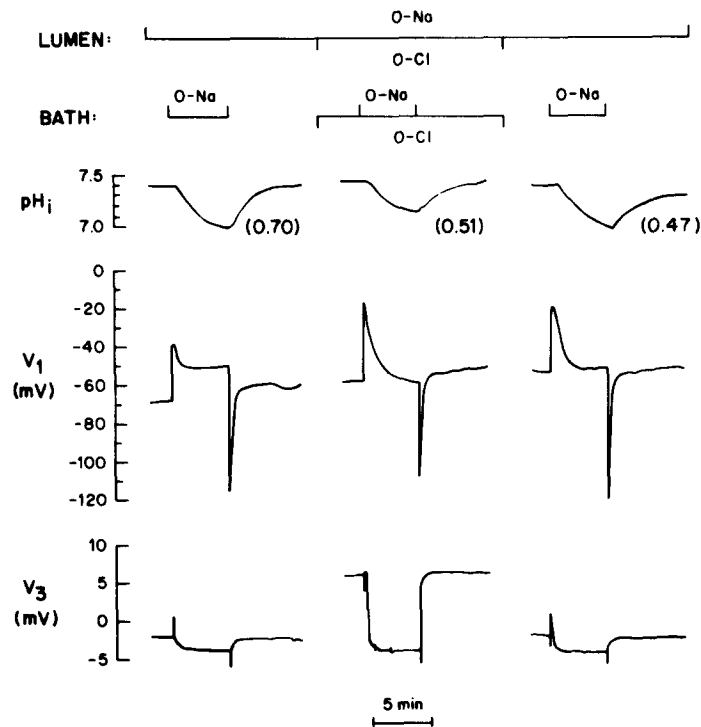


FIGURE 12. Effect of Cl^- removal on pH_i and voltage changes induced by alterations of $[Na^+]_b$. V_1 and V_3 represent basolateral membrane potential and transepithelial potential, respectively. Basolateral Na^+ is removed (replaced by NMDG $^+$) during three different intervals. 12 min before the second 0-Na interval, Cl^- was removed (replaced by glucuronate) from both the bath and lumen. The first gap in the record represents 8.3 min, the second represents 25 min. Throughout the experiment, pH was 7.5 and solutions were buffered with 10 mM $HCO_3^-/1.5\%$ CO_2 . A total of 13 similar experiments was performed on 5 separate tubules.

Na^+ removal. The initial rate of a_i^{Cl} rise (i.e., over the first 40 s) is 2.1 mM/min. This contrasts with an initial equivalent HCO_3^- flux of 12.6 mM/min calculated from Fig. 9 under identical conditions. During the first 140 s of basolateral Na^+ removal, a period sufficient for the accompanying pH_i fall to be complete (Fig. 9), a_i^{Cl} rises by a total of 3.9 mM. In this same time interval in Fig. 9, the equivalent loss of HCO_3^- was 10.9 mM. This latter figure is a

minimal estimate, since the pH_i decline is blunted by luminal Na-H exchange. After the first 140 s, however, a_i^{Cl} continues to rise, achieving a total increase of 8.2 mM after ~ 7 min. Thus, because of the large discrepancy between the initial Cl^- flux and the initial equivalent HCO_3^- flux, as well as the substantial

TABLE V
 Cl^- DEPENDENCE OF pH_i RECOVERY AFTER RETURNING
 BASOLATERAL Na^+ *

Tubule	k_{HCO_3}	$k_{0\text{-Cl}}$	$k_{0\text{-Cl}}/k_{\text{HCO}_3}$
071481	0.51 ± 0.07 (2)	0.46 ± 0.08 (4)	0.89
071581	0.53 ± 0.09 (3)	0.48 ± 0.03 (2)	0.90
071681	0.74 ± 0.02 (2)	0.74 ± 0.05 (3)	1.00
071781A	1.56 ± 0.14 (2)	1.54 ± 0.04 (2)	0.98
071781B	<u>1.13</u> (1)	<u>0.75 ± 0.05</u> (2)	<u>0.67</u>
	0.91 ± 0.17	0.85 ± 0.17	0.91

* k_{HCO_3} is the rate constant in Cl-containing HCO_3^- Ringer; $k_{0\text{-Cl}}$ is the rate constant in Cl-free HCO_3^- Ringer. The mean k_{HCO_3} is not significantly different from the mean $k_{0\text{-Cl}}$ (paired t test; $P = 0.36$). The mean $k_{0\text{-Cl}}/k_{\text{HCO}_3}$ was obtained assuming a log-normal distribution. The number of experiments per tubule given in parentheses. Luminal solutions were all Na-free so that the pH_i recoveries were minimally contaminated by luminal events.

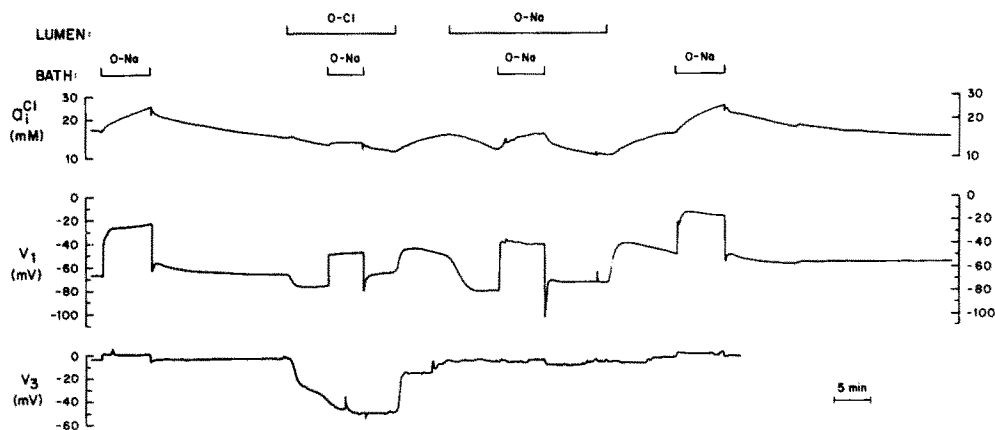


FIGURE 13. Intracellular Cl^- activity during changes in $[\text{Na}^+]_b$. V_1 and V_3 represent basolateral membrane potential and transepithelial potential, respectively. During the first interval of basolateral Na^+ removal, both Na^+ and Cl^- were present in the lumen. During the second, Cl^- was absent from the lumen only. During the third 0- $[\text{Na}^+]_b$ interval, Na^+ was absent from the lumen. Finally, during the fourth interval, both Na^+ and Cl^- were present in the lumen. Throughout the experiment, pH was 7.5 and solutions were buffered with 10 mM $\text{HCO}_3^-/1.5\%$ CO_2 . A total of six similar experiments, incorporating one or more elements of Fig. 13, was performed, each on a separate tubule.

difference in the overall time course of a_i^{Cl} and pH_i , the basolateral equivalent HCO_3^- flux cannot all be linked to Cl^- . The subsequent return of Na^+ to the basolateral solution causes a_i^{Cl} to return to about its initial value over a period

of ~20 min, which indicates once again a discrepancy between the time courses of Cl^- and equivalent HCO_3^- fluxes, because the pH_i recovery is essentially complete in 2–3 min.

Several mechanisms might be invoked to explain the observed rise in a_i^{Cl} in the experiment of Fig. 13. (i) Basolateral or luminal Cl-HCO_3 (or Cl-OH) exchange cannot account for the rise of a_i^{Cl} , since the observed fall of pH_i could only serve to reduce Cl^- influx. (ii) A basolateral, electroneutral $\text{Na/HCO}_3\text{-Cl/H}$ exchange, such as identified in invertebrate nerve and muscle, could account for the rise of a_i^{Cl} . Indeed, such a transporter has been postulated to account for Cl^- transport across the basolateral membrane of the *Necturus* proximal tubule (Guggino et al., 1982). And finally, (iii) the increase of a_i^{Cl} could result in part from an entry of Cl^- across the luminal membrane. For example, if lowering $[\text{Na}^+]_b$ reduces a_i^{Na} , as is known to be the case (Sackin et al., 1981), then Cl^- would be expected to enter across the luminal membrane via an electroneutral NaCl cotransporter.

To test this last possibility, we moved from the lumen either Cl^- or Na^+ and repeated the basolateral Na^+ removal experiment (Fig. 13). The luminal removal of Cl^- produces a slow fall of a_i^{Cl} . During this period of declining a_i^{Cl} , we removed basolateral Na^+ and found that a_i^{Cl} increased by only ~0.6 mM after 5 min. Correcting for the declining a_i^{Cl} baseline, the true increase in a_i^{Cl} is probably closer to 1.0 mM, substantially less than the rise of a_i^{Cl} that occurred in a comparable time under control conditions, 6.3 mM. Some of this depression of the a_i^{Cl} increase is probably due to the absence of unidirectional Cl^- influx via a luminal NaCl cotransporter. To further test this possibility, we returned Cl^- to the lumen (note the rise in a_i^{Cl}) and subsequently removed Na^+ from the lumen (note the fall in a_i^{Cl}). When Na^+ is now removed from the bath, in the absence of luminal Na^+ , a_i^{Cl} increases by 3.9 mM after ~7 min (correcting for the declining a_i^{Cl} baseline), which is substantially less than after a comparable time under control conditions, 8.2 mM. The inability of luminal Na^+ removal to completely inhibit the rise of a_i^{Cl} suggests that there is another mode of Cl^- entry besides luminal NaCl cotransport. Moreover, the leveling off of this rise in a_i^{Cl} , as opposed to the continuing rise under control conditions, suggests a mechanism of Cl^- entry that is limited by the depletion of intracellular Na^+ . This could well be basolateral $\text{Na/HCO}_3\text{-Cl/H}$ exchange.

Finally, Na^+ is returned to the lumen, causing a slow rise of a_i^{Cl} , which may reflect the activity of a luminal NaCl cotransporter. When Na^+ is subsequently removed from the basolateral solution, as in the initial control experiments, a_i^{Cl} again increases. The rise amounts to 9.6 mM over ~7 min, comparable to the previous value, 8.2 mM. Similarly, the return of Na^+ to the bath leads to a slow recovery of a_i^{Cl} .

DISCUSSION

Basolateral HCO_3^- Transport

In the preceding paper (Boron and Boulpaep, 1983), we showed that the salamander proximal tubule cell possesses Na-H exchangers on both the luminal and basolateral membranes. The cell must, of course, have some

asymmetry of its H^+ and/or HCO_3^- transporters if it is to engage in net, transcellular acid secretion. The results of the present study show that the requisite asymmetry of the tubule cell, with respect to acid transport, is conferred by a pathway for HCO_3^- (or an equivalent species), which is confined to the basolateral membrane. Evidence for a basolateral pathway for HCO_3^- movement comes from three observations in the experiment of Fig. 1. (i) Application of CO_2/HCO_3^- Ringer causes a fall in pH_i from which the cell fails to recover. Although the CO_2 -induced fall in pH_i undoubtedly stimulates Na-H exchange, this increased rate of acid extrusion is balanced by the newly established efflux of HCO_3^- and/or a related species. (ii) Reducing pH_b causes a much larger fall in pH_i when the basolateral solution contains HCO_3^- (at constant pCO_2) than when it is nominally HCO_3^- free. (iii) In HCO_3^- Ringer, reducing pH_b at constant pCO_2 has a substantially larger effect on pH_i than reducing pH_i , which indicates that the pathway for HCO_3^- must be limited to the basolateral membrane.

Although the changes in pH_i induced by changes in $[HCO_3^-]_b$ are indicative of a basolateral pathway for HCO_3^- (or an equivalent species), this pathway is not the sole contributor to the pH_i changes in the aforementioned experiments. In fact, the decline in pH_i produced by lowering $[HCO_3^-]_b$ and pH_b (at constant pCO_2) probably has two major causes: (i) a reduction in the basolateral Na-H exchange rate in the face of continued intracellular acid loading, and (ii) an increased net efflux of HCO_3^- and/or a related species. Similarly, returning $[HCO_3^-]_b$ and pH_b to normal produces a very rapid recovery of pH_i , which apparently has two major components: (i) an increased rate of basolateral Na-H exchange, and (ii) an influx of HCO_3^- and/or a related species. The contribution of Na-H exchange is clearly demonstrated by the inhibitory effect of amiloride on the pH_i recovery (see Fig. 2). The component of the pH_i recovery remaining after application of amiloride, which largely blocks Na-H exchange, is presumably due to basolateral HCO_3^- transport.

The transport of HCO_3^- (or of an equivalent species) across the basolateral membrane could theoretically be effected by any of the five transport mechanisms listed in Fig. 14. The following observations must be accounted for: (i) pH_i falls when $[HCO_3^-]_b$ is lowered from 10 to 2 mM (i.e., pH_b is lowered from 7.5 to 6.8), and rises when the reverse solution change is made. (ii) a_i^{Na} falls when $[HCO_3^-]_b$ is lowered, and rises when the reverse solution change is made. (iii) The basolateral membrane depolarizes, usually transiently, upon reducing $[HCO_3^-]_b$, and hyperpolarizes, always transiently, upon restoring $[HCO_3^-]_b$ to a normal level. (iv) There are only small changes in a_i^{Cl} when $[HCO_3^-]_b$ is altered. (v) pH_i falls when $[Na^+]_b$ is reduced to zero and rises when $[Na^+]_b$ is raised to normal. (vi) a_i^{Na} correspondingly falls and rises when $[Na^+]_b$ is altered. (vii) The basolateral membrane transiently depolarizes upon reduction of $[Na^+]_b$ and transiently hyperpolarizes upon restoration of $[Na^+]_b$. (viii) Changes in a_i^{Cl} induced by alterations in $[Na^+]_b$ appear not to be directly related to the aforementioned changes in pH_i , a_i^{Na} , or V_1 . (ix) The aforementioned changes in pH_i , a_i^{Na} , and V_1 are blocked by SITS, but are not inhibited by removal of Cl^- .

Each of the five models is examined in detail for the six most important experimental conditions of the Results. The first three conditions pertain to the experiment in which $[\text{HCO}_3^-]_b$ is reduced (as in Fig. 1C), and the final three pertain to the experiment in which $[\text{Na}^+]_b$ is reduced (as in Fig. 7A): (i) the standard control condition, (ii) at the instant $[\text{HCO}_3^-]_b$ is reduced from 10 to 2 mM, (iii) at the instant $[\text{HCO}_3^-]_b$ is restored to 10 mM, (iv) the new control condition in which $[\text{Na}^+]_i$ is 0 mM, (v) at the instant $[\text{Na}^+]_b$ is reduced from 100 to 0 mM, and (vi) at the instant $[\text{Na}^+]_b$ is restored to 100 mM.

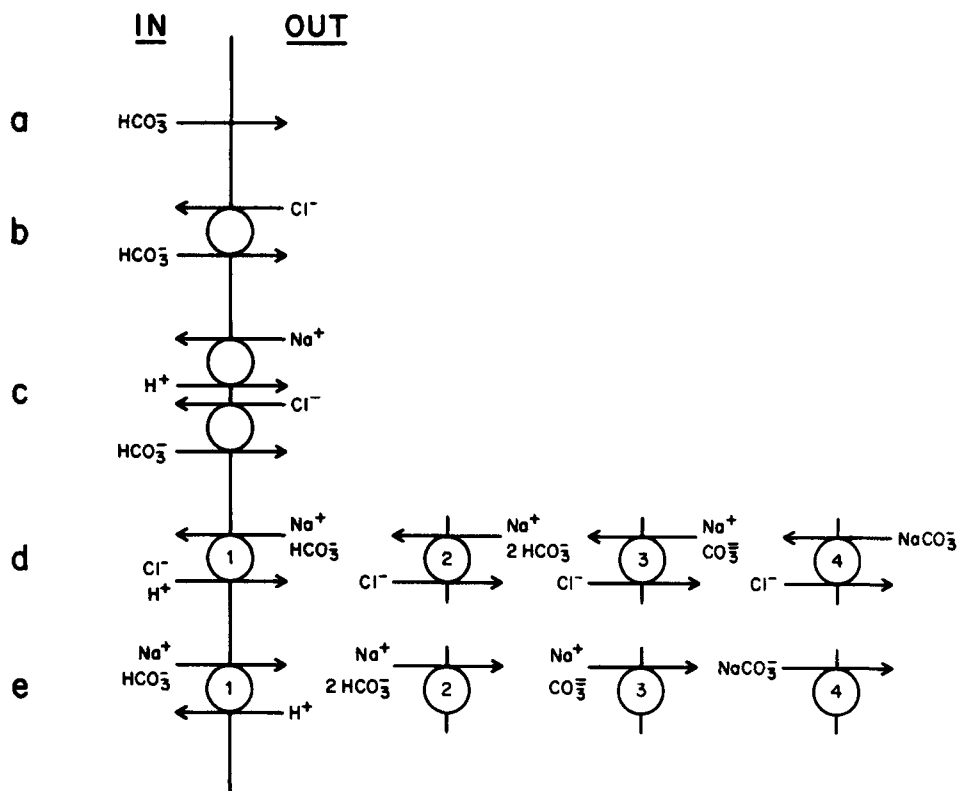


FIGURE 14. Five models for basolateral HCO_3^- transport.

These conditions, and the ion activities and voltages pertaining to them, are summarized in Table VI for each of the five models of Fig. 14. The Appendix contains the thermodynamic calculations necessary for determining whether each of the models can account for the observed changes of intracellular ion activities and voltages for each of the six aforementioned conditions.

(a) *Conductive path for HCO_3^- .* As shown in the Appendix, a simple conductive path for HCO_3^- can account for the presumed efflux of HCO_3^- (or an equivalent species) in the control condition *i* and is consistent with the observations for condition *iv*, but cannot account by itself for the pH_i changes in conditions *ii*, *iii*, *v*, or *vi*. A small basolateral conductance for HCO_3^- cannot

be ruled out. However, as indicated in the Results, the observed resting V_1 as well as the V_1 changes induced by alterations of $[\text{HCO}_3^-]_b$ are not consistent with a high partial conductance for HCO_3^- .

(b) *Cl-HCO₃ exchange.* As shown in the Appendix, an electroneutral Cl-HCO₃ exchanger could account for the observations in conditions *i*, *ii*, and *iv*, but cannot explain the activity changes occurring during conditions *iii*, *v*, and *vi*. Furthermore, since it predicts electroneutrality, it also cannot explain the observed changes in V_1 induced by altering either $[\text{HCO}_3^-]_b$ or $[\text{Na}^+]_b$. Although we cannot rule out a small component of Cl-HCO₃ exchange, we conclude that this process cannot by itself account for our data.

(c) *Na-H exchange in parallel with Cl-HCO₃ exchange.* As detailed in the Appendix, the parallel exchanger model makes an indeterminate prediction concerning conditions *i* and *iv*, and would satisfy condition *v*, but cannot account for the activity changes of conditions *ii*, *iii*, and *vi*. Furthermore, parallel exchangers cannot account for the observed voltage changes. We conclude that this hypothesis cannot by itself account for the data. Note, however, that basolateral Na-H has been identified in this preparation (Boron and Boulpaep, 1983).

Inasmuch as several investigators have suggested that electroneutral NaCl entry at the luminal membrane is mediated by parallel Na-H and Cl-HCO₃ exchangers, it is instructive to analyze the thermodynamic predictions of such a hypothesis. The free-energy changes for luminal Na-H and Cl-HCO₃ exchangers are the same as those noted above for basolateral exchangers in the control condition *i*: the ΔG_{net} for both exchangers is such that net Na⁺ and Cl⁻ entry would occur at the luminal membrane. Thus, the parallel exchange model can at least qualitatively account for luminal NaCl uptake. Only in the fortuitous case in which overall transport is isohydric, however, would Na⁺ and Cl⁻ move in equimolar amounts. The results of two additional experiments, performed by others on the *Necturus* proximal tubule (Spring and Kimura, 1978; Kimura and Spring, 1979) and by us in the present study, provide the basis for a more detailed examination of the parallel exchanger model. In one experiment $[\text{Cl}^-]_l$ only was lowered, and in the other, $[\text{Na}^+]_l$ only. In both cases, however, a_i^{Cl} and a_i^{Na} both fall. This linkage between Cl⁻ and Na⁺ could be achieved in any of four ways: (*i*) a direct linkage at the luminal membrane (e.g., NaCl cotransport), (*ii*) an indirect linkage at the luminal membrane (e.g., parallel Na-H and Cl-HCO₃ exchangers linked by changes in pH_i), (*iii*) a direct linkage at the basolateral membrane, and (*iv*) an indirect linkage at the basolateral membrane. The a_i^{Cl} and a_i^{Na} decreases in the aforementioned two experiments are certainly consistent with mechanisms *i* and *iv*. Possibility *ii* cannot account for the data because the requisite pH_i changes do not occur. For example, lowering $[\text{Cl}^-]_l$ could reverse a Cl-HCO₃ exchanger (Cl⁻ out, Na⁺ in), but could not reverse the Na-H exchanger (Na⁺ out, H⁺ in) unless pH_i would rise above 7.99. Although we have yet to lower $[\text{Cl}^-]$ in the lumen only, simultaneously removing Cl⁻ from lumen and bath caused pH_i to fall or remain unchanged. Conversely, lowering $[\text{Na}^+]_l$ could reverse a Na-H exchanger, but could not reverse a Cl-HCO₃ exchanger unless pH_i would fall below 6.85. Fig. 7B shows that luminal Na⁺ removal causes

only a transient fall of pH_i by 0.1 to a value of ~ 7.2 ; the steady state pH_i is unchanged. Possibility *iii* also cannot explain the data. It predicts that lowering $[\text{Cl}^-]_i$ should reduce a_i^{Cl} but raise a_i^{Na} , and that lowering $[\text{Na}^+]_i$ should lower a_i^{Na} but raise a_i^{Cl} . Such increases in a_i^{Na} and a_i^{Cl} have not been observed. These data do not rule out parallel Na-H and Cl-HCO₃ exchangers at the luminal membrane. However, they indicate that the simultaneous reversal of such exchangers cannot account for the decreases of a_i^{Cl} and a_i^{Na} observed when either $[\text{Cl}^-]_i$ or $[\text{Na}^+]_i$ is reduced.

(*d*) *Na/HCO₃-Cl/H exchange.* In squid axons (Russell and Boron, 1982), snail neurons (Thomas, 1977), and barnacle muscle (Boron et al., 1979, 1981), pH_i is regulated by a system that exchanges external HCO₃⁻ and Na⁺ for internal Cl⁻ (and possibly H⁺). The stoichiometry is one Na⁺ entering for each Cl⁻ leaving, and each pair of protons neutralized intracellularly (Russell and Boron, 1982). Thomas (1977) has suggested model *d1* of Fig. 14. This is not distinguishable thermodynamically from models *d2-d4*, which are also presented.

As detailed in the Appendix, this model fails to account for our observations for all experimental conditions other than *iv*. Note, however, that the discrepancies for conditions *ii*, *iii*, *v*, and *vi* all bear on the involvement of Cl⁻. We recognize that the transporter could have such a high affinity for Cl⁻ that it could be difficult to demonstrate a Cl⁻ dependence, and that a_i^{Cl} could be so well regulated by other transport systems that large changes of a_i^{Cl} would not occur. However, even if the interpretation of the Cl⁻ data were in error, this electroneutral model would still fail to explain the voltage changes. We conclude that an Na/HCO₃-Cl/H exchanger cannot by itself account for our data, though we cannot rule out the participation of such an exchanger in the a_i^{Cl} shifts.

(*e*) *Electrogenic Na/HCO₃ transport.* Fig. 14 lists four thermodynamically indistinguishable variants that would result in the equivalent of electrogenic Na/HCO₃ transport. Although the stoichiometry predicted by these models is equivalent to two HCO₃⁻ for each Na⁺, we emphasize that our data only require that the ratio of net fluxes of HCO₃⁻ to Na⁺ be greater than unity. Models *e1-e4* are the same as *d1-d4*, except for the lack of Cl⁻ involvement. As described in the Appendix, models *e1-e4* account for all the a_i^{Na} and pH_i data for the six experimental conditions. The models also account for all V_1 transients that follow changes in $[\text{HCO}_3^-]_b$ and $[\text{Na}^+]_b$, as well as the depolarization accompanying application of CO₂/HCO₃⁻ Ringer.

The reversal potential for the electrogenic Na/HCO₃ transport system is the equilibrium potential for the anion pair in model *e4*, E_{NaCO_3} :

$$E_{\text{NaCO}_3} = \frac{RT}{F} \ln \frac{[\text{Na}^+]_i [\text{HCO}_3^-]_i^2}{[\text{Na}^+]_o [\text{HCO}_3^-]_o^2}$$

The values of ΔG described in the Appendix are related to E_{NaCO_3} by the equation

$$\Delta G = F(V_1 - E_{\text{NaCO}_3}).$$

It is instructive to examine the relationship between E_{NaCO_3} and V_1 for each of the six experimental conditions described above. (i) In the normal control condition, E_{NaCO_3} is -52.4 mV, compared with a V_1 in HCO_3^- Ringer of about -60 mV. Thus, the transport system would carry negative current outward and thereby tend to depolarize the basolateral membrane. This explains why the basolateral membrane depolarizes when the tubule is transferred from HEPES to HCO_3^- Ringer (i.e., from solution 9 to 1). (ii) When $[\text{HCO}_3^-]_b$ is reduced to 2 mM, E_{NaCO_3} instantly becomes $+29.3$ mV, explaining the observed, basolateral depolarization. (iii) When $[\text{HCO}_3^-]_b$ is subsequently restored to 10 mM, E_{NaCO_3} instantly becomes -98.2 mV, which accounts for the observed basolateral hyperpolarization. (iv) In the new control condition (with a $[\text{Na}^+]_i$ of 0 mM), E_{NaCO_3} is -72.2 mV close to the prevailing value of V_1 (approximately -70 mV). (v) When $[\text{Na}^+]_b$ is reduced to 0 mM, E_{NaCO_3} instantly approaches $+\infty$, accounting for the abrupt basolateral depolarization. (vi) When $[\text{Na}^+]_b$ is subsequently returned to 100 mM, E_{NaCO_3} instantly becomes -151.1 mV, which again explains hyperpolarizations of the basolateral membrane which, in some cases, reached -140 mV.

If the electrogenic Na/HCO_3^- transporter is indeed responsible for a portion of the pH_i and V_1 changes associated with the alteration of either $[\text{HCO}_3^-]_b$ or $[\text{Na}^+]_b$, then the magnitude of a V_1 change should be related in a predictable way to the rate of pH_i change. Consider as an example the experiment of Fig. 7A, in which Na^+ is removed from and then returned to the bath. The rate of pH_i recovery upon restoring Na^+ to the bath is ~ 0.014 pH units $\cdot \text{s}^{-1}$. If the pH_i recovery is due entirely to the entry of HCO_3^- and Na^+ in a 2:1 ratio, then it can be shown⁶ that the expected initial basolateral hyperpolarization is 34 mV. This value should be interpreted with caution since, on the one hand, the rather slowly responding pH microelectrode probably underestimates the very rapid, initial pH_i recovery rate, while on the other, a portion of the pH_i recovery is probably due to electroneutral $\text{Na}-\text{H}$ exchange. Assuming that these opposing influences approximately cancel each other, then the calculated hyperpolarization is in reasonable agreement with that actually observed,⁷ 38 mV. Thus, it would seem that a single Na/HCO_3^- transporter could account for both the V_1 and pH_i changes

With the present data, we cannot distinguish among models *e1-e4*. The last

⁶ The product of this pH_i recovery rate (i.e., 0.014 pH $\cdot \text{s}^{-1}$) and the total intracellular buffering power at $\text{pH}_i = 7.0$ (i.e., 43 mM/pH; see Boron and Boulpaep, 1983) is the equivalent net influx of HCO_3^- across the basolateral membrane, 0.602 mmol $\cdot \text{s}^{-1} \cdot (\text{liter cell volume})^{-1}$. If the stoichiometry is two HCO_3^- for each Na^+ , this corresponds to a flux of 0.301 meq $\cdot \text{s}^{-1} \cdot (\text{liter cell volume})^{-1}$, or to 29.0 amp $\cdot (\text{liter cell volume})^{-1}$. The ratio of cell volume to luminal surface area for the *Ambystoma* proximal tubule is 2.54×10^{-3} cm, based on a morphometric analysis (Maunsbach and Boulpaep, unpublished). Thus, the current flow through the Na/HCO_3^- transporter would be 73.7 $\mu\text{A} \cdot \text{cm}^{-2}$. Given a transepithelial resistance for the *Ambystoma* of 52.1 $\Omega \cdot \text{cm}^2$ (Sackin and Boulpaep, 1981a), a basolateral membrane resistance of 591 $\Omega \cdot \text{cm}^2$ (Sackin et al., 1982), and a luminal membrane resistance of $2,305$ $\Omega \cdot \text{cm}^2$ (Sackin and Boulpaep, unpublished), then the calculated basolateral hyperpolarization (taking current loops into account), comes to 34 mV.

⁷ The magnitude of the hyperpolarization is taken as the degree to which V_1 transiently undershoots the final steady state V_1 . This is the portion which is blocked by SITS.

one, a channel or a carrier for the ion pair, is perhaps the simplest inasmuch as only a single species need cross the membrane. NaCO_3^- is known to exist, though its expected concentration is very low. The data of Garrels et al. (1961), which were obtained for seawater and therefore can provide only a rough estimate, predict a $[\text{NaCO}_3^-]_b$ of only $\sim 25 \mu\text{M}$. This would require a carrier of high affinity or a channel of extraordinary permeability.

Unifying Model for Basolateral Na^+ , HCO_3^- , and Cl^- Transport

The simultaneous, transcellular reabsorption of HCO_3^- and Cl^- requires the basolateral efflux of both HCO_3^- and Cl^- . The present study documents an electrogenic Na/HCO_3 transporter capable of high transport rates, and which carries most of the HCO_3^- and a fraction of the Na^+ out across the basolateral membrane. The mechanism of Cl^- efflux at the basolateral membrane is unsettled. Basolateral Cl^- conductance in the *Necturus* proximal tubule is probably too low (Guggino et al., 1982) to mediate the efflux, and an electroneutral $\text{Cl}-\text{HCO}_3$ exchanger would normally be poised in the direction of basolateral Cl^- entry. However, Guggino et al. (1980) have identified a basolateral Cl^- transporter with properties expected of model *d* of Fig. 14. As is evident from the analyses in the Appendix, independent Cl^- and HCO_3^- systems are a necessity for the simultaneous basolateral efflux of Cl^- and HCO_3^- . However, the electrogenic Na/HCO_3 transporter shares several characteristics with the postulated Cl^- system: (i) involvement of Na^+ , (ii) involvement of HCO_3^- , and (iii) sensitivity to SITS. We suggest a scheme (Fig. 15) in which a single carrier could accomplish the two apparently disparate tasks. The upper loop in Fig. 15, described by the directions k_1 and k_{-2} , represents the hypothesized electrogenic Na/HCO_3 transporter operating in the direction of HCO_3^- reabsorption. The large loop, in the direction described by k_{-1} and k_3 , represents the $\text{Na}/\text{HCO}_3-\text{Cl}/\text{H}$ exchanger operating in the direction of a classic pH_i regulator (i.e., Cl^- reabsorption). The lower loop, in the direction described by k_3 and k_{-2} , is equivalent to an electrogenic Cl^- carrier operating in the direction of Cl^- reabsorption. All three loops have been described in the directions appropriate for exergonic reactions under normal conditions. Depending upon the values chosen for the various rate constants, this system could mediate pure Na/HCO_3 reabsorption, pure Cl^- reabsorption, any combination of the two, or even Cl^- reabsorption with the opposite movement of Na/HCO_3 . When concentrations or voltages are altered, the net directions of one or more loops could be reversed and thereby produce a wide variety of apparent interdependencies among the fluxes of the ions and net negative charge.

Model of Renal Acid Secretion

Nerve and muscle cells actively regulate their pH_i by extruding acid from the cell (Roos and Boron, 1981). The rate of acid extrusion in barnacle muscle approaches zero at pH_i values at or above a certain threshold, and gradually increases as pH_i falls below this threshold. The $\text{Na}-\text{H}$ exchanger of the proximal tubule cells apparently exhibits a similar sensitivity to intracellular

acid loading, regulating pH_i much as it would in a nerve or muscle cell (Boron and Boulpaep, 1983). In the absence of a basolateral pathway for HCO_3^- (as can be achieved by nominal removal of HCO_3^- , or by addition of SITS), the tubule cells function much the same as a nerve or muscle cell with respect to pH_i regulation. It is basolateral HCO_3^- transport that endows these cells with the potential for transcellular acid secretion. It should be noted that acid secretion has yet to be demonstrated in this tubule segment. Nevertheless, the identification of HCO_3^- and H^+ transport systems in this and the companion study (Boron and Boulpaep, 1983), makes it likely that such acid secretion

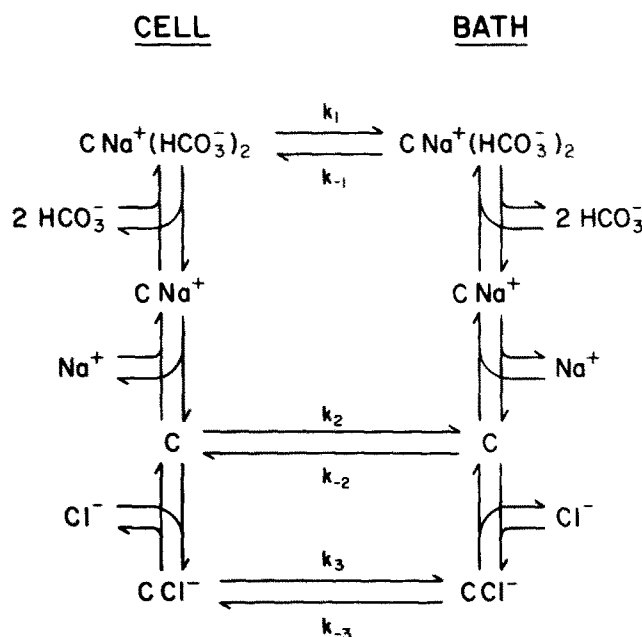


FIGURE 15. Model accounting for basolateral HCO_3^- and Cl^- transport on the basis of a single carrier. This simplified scheme, based on mechanisms $d2$ and $e2$ of Fig. 14, is not meant to imply a detailed kinetic model. It could be expanded to include all the rate constants and to specify a precise mode of binding of the multiple ligands. The model also permits SITS-sensitive Na-Na and Cl-Cl exchanges.

can indeed occur. In the control state, there is a net efflux of Na/ HCO_3^- across the basolateral membrane. This efflux lowers pH_i and a_i^{Na} and therefore stimulates the pH_i -regulating mechanism: luminal and basolateral Na-H exchange. The extrusion of H^+ across the basolateral membrane represents a substantial inefficiency with respect to the presumed acid secretory activity of the tubule, since this extrusion short-circuits a portion of the basolateral HCO_3^- efflux. H^+ extrusion across the luminal membrane is identical to the presumed unidirectional, transcellular acid secretion.

Our model of proximal-tubule acid secretion represents a unifying theory

of intracellular pH regulation in epithelial and nonepithelial cells. However, it differs somewhat from the prevailing viewpoint, which has luminal acid extrusion (and therefore a rise in pH_i) as the primary event in acid secretion, and the basolateral HCO_3^- efflux merely following to keep pH_i from rising too high. Cited as evidence for this latter view is the observation that pH_i in proximal tubule cells is rather alkaline, ~ 7.4 . The crucial parameter, however, is not the absolute value of the steady state pH_i , but rather the degree to which pH_i is below the threshold for activating the pH_i -regulating mechanism. We estimate that the pH_i threshold of the proximal tubule cells' Na-H exchanger is at or somewhat above 7.43, the mean pH_i in HEPES Ringer (Boron and Boulpaep, 1983). In the absence of basolateral HCO_3^- efflux, the rate of intracellular acid loading is probably very low in these amphibian cells, and the unopposed pH_i -regulating system (i.e., the Na-H exchangers) drives pH_i upward to ~ 7.43 , at which point the Na-H exchangers are, or are nearly, inactive. The normal pH_i of these cells at a physiologic $[\text{HCO}_3^-]_b$ and pCO_2 , however, is ~ 0.17 lower than 7.43. This represents a substantial intracellular acid load, which must therefore greatly stimulate Na-H exchange. Thus, we feel that the primary event in acid secretion is the basolateral efflux of HCO_3^- , which decreases pH_i below the threshold for activating the pH_i -regulating mechanism. For the salamander, in which basolateral HCO_3^- transport is mediated by the Na/ HCO_3^- transporter (see Fig. 16), basolateral HCO_3^- efflux is also accompanied by a fall in a_i^{Na} , which may also enhance Na-H exchange. The rate of transcellular acid secretion (i.e., luminal Na-H exchange) is therefore directly regulated by pH_i and, to a certain extent, a_i^{Na} . We predict that the proximal tubule's rate of transcellular acid secretion should be increased by any treatment which lowers pH_i : raising pCO_2 (at constant external pH), lowering $[\text{HCO}_3^-]_b$ (at constant pH_i), and selectively inhibiting basolateral Na-H exchange.

APPENDIX

Thermodynamic Analysis of Basolateral HCO_3^- Transport

The hypothetical movements of the HCO_3^- (or an equivalent species) can be analyzed for six relevant experimental conditions. The first three pertain to the experiment in which $[\text{HCO}_3^-]_b$ is reduced (see Fig. 1C), and the final three pertain to the experiment in which $[\text{Na}^+]_b$ is reduced (see Fig. 7A): (i) the control condition, (ii) at the instant $[\text{HCO}_3^-]_b$ is reduced from 10 to 2 mM, (iii) at the instant $[\text{HCO}_3^-]_b$ is restored to 10 mM, (iv) the new control condition in which $[\text{Na}^+]_i$ is 0 mM, (v) at the instant $[\text{Na}^+]_b$ is reduced from 100 to 0 mM, and (vi) at the instant $[\text{Na}^+]_b$ is restored to 100 mM. These conditions are summarized in Table VI.

CONDUCTIVE PATH FOR HCO_3^- The net free energy change for HCO_3^- as it exits across the basolateral membrane is:

$$\Delta G_{\text{net}} = RT \ln \frac{[\text{HCO}_3^-]_b}{[\text{HCO}_3^-]_i} + FV_1,$$

where $\Delta G_{\text{net}} < 0$ indicates a net HCO_3^- efflux. In addition, the HCO_3^- flux through an idealized channel can be calculated from the constant field equation (Goldman, 1943;

Hodgkin and Katz, 1949):

$$J_{\text{HCO}_3}^{\text{net}} = P \cdot \frac{V_1 F}{RT} \cdot \frac{[\text{HCO}_3^-]_b - [\text{HCO}_3^-]_i \epsilon}{1 - \epsilon},$$

where $J_{\text{HCO}_3}^{\text{net}}$ is the net HCO_3^- influx; P is the permeability to HCO_3^- ; F , R , and T have their usual meanings; and $\epsilon = \exp(-V_1 F/RT)$. (i) Under standard control conditions (see Table VI), ΔG_{net} is $-1.9RT$ and $J_{\text{HCO}_3}^{\text{net}}$ comes to $-14.0 P$ (units: $10^{-6} \text{ mol cm}^{-2} \text{ s}^{-1}$); the negative signs signify a net efflux. This is in agreement with the

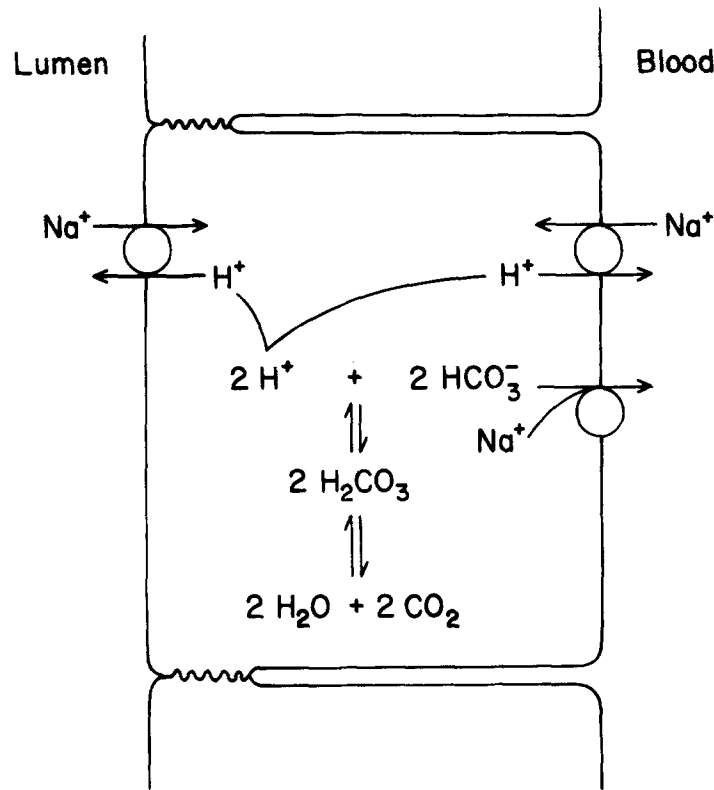


FIGURE 16. Model of acid secretion in the salamander proximal tubule.

sustained fall in pH_i , presumably because of the net efflux of HCO_3^- (or an equivalent species), actually observed when HCO_3^- -free is replaced with HCO_3^- -containing Ringer (see Fig. 1A). (ii) When $[\text{HCO}_3^-]_b$ is reduced from 10 to 2 mM, there is an immediate basolateral depolarization of ~ 20 mV. The instantaneous ΔG_{net} is therefore $-2.7RT$, which predicts an increased gradient for HCO_3^- efflux. The calculated, instantaneous $J_{\text{HCO}_3}^{\text{net}}$, however, is actually reduced somewhat to $-11.7P$. This occurs because V_1 appears as an exponential term in the expression for $J_{\text{HCO}_3}^{\text{net}}$, causing the effect of the depolarization to outweigh that of lowering $a_b^{\text{HCO}_3^-}$.] Therefore, unless P increases substantially as pH_b is reduced from 7.5 to 6.8, the observed fall in pH_i cannot be explained by an increased passive HCO_3^- efflux. (iii) Just before $[\text{HCO}_3^-]_b$ is returned to 10 mM, $a_i^{\text{HCO}_3^-}$ is 2.1 mM (assuming that pH_i had previously fallen by 0.35). When $[\text{HCO}_3^-]_b$ is raised, V_1 instantly hyperpolarizes to about -60 mV. The initial ΔG_{net} is $-1.1RT$, which predicts a continued net HCO_3^- efflux. The initial

$J_{\text{HCO}_3}^{\text{net}}$ comes to $-4.8P$, a net efflux which would be smaller than that prevailing during the reduction of $[\text{HCO}_3^-]_b$ (condition *ii*), but not the net influx required to explain the data. (*iv*) In the new control condition in which $[\text{Na}^+]_i$ is 0 mM, the basolateral membrane is hyperpolarized compared with condition *i*, and V_1 will be assumed to be -70 mV. ΔG_{net} comes to $-2.3RT$ and predicts a net efflux. $J_{\text{HCO}_3}^{\text{net}}$ is $-16.7P$, describing the magnitude of this efflux. The data of Fig. 7B are consistent with a diminished net HCO_3^- efflux or even an influx. (*v*) When $[\text{Na}^+]_b$ is reduced to

TABLE VI
PREDICTED FREE ENERGY CHANGES FOR FIVE MODELS OF BASOLATERAL
 HCO_3^- TRANSPORT* AND PARAMETER VALUES ASSUMED IN
CALCULATIONS‡

Model	ΔG values					
	$[\text{Na}^+]_i = 100$ mM			$[\text{Na}^+]_i = 0$ mM		
	(i) Control	(ii) $[\text{HCO}_3^-]_b$	(iii) $[\text{HCO}_3^-]_b$	(iv) Control	(v) $[\text{Na}^+]_b$	(vi) $[\text{Na}^+]_b$
(a) HCO_3^-	$-1.9RT$	$-2.7RT$	$-1.1RT$	$-2.3RT$	$-0.7RT$	$-2.7RT$
(b) Cl- HCO_3^-	-1.0	-2.6	0.0	-1.0	-1.0	0.0
(c) Na-H	-1.6	0.0	-2.6	-2.4	$+\infty$	-4.7
Cl- HCO_3^-	-1.0	-2.6	0.0	-1.0	-1.0	0.0
(d) Na/ HCO_3^- -Cl/H	-0.6	+2.6	-2.5	-1.4	$+\infty$	-4.7
(e) Na/ HCO_3^-	-0.3	-2.7	+1.5	-0.1	$-\infty$	+2.0
Parameters	Parameter values					
pH _i	7.30	7.30	6.95	7.30	7.30	6.95
pH _b	7.50	6.80	7.50	7.50	7.50	7.50
	mM	mM	mM	mM	mM	mM
$a_i^{\text{HCO}_3^-}$	4.7	4.7	2.1	4.7	4.7	2.1
$a_o^{\text{HCO}_3^-}$	7.5	1.5	7.5	7.5	7.5	7.5
a_i^{Na}	24	24	20	11	11	2.5
a_b^{Na}	75	75	75	75	0	75
a_i^{Cl}	16	16	19	16	16	20
a_b^{Cl}	71	71	71	71	71	71
V_1	$-0.060V$	$-0.040V$	$-0.060V$	$-0.070V$	$-0.030V$	$-0.100V$

* The reactions are written so that they proceed spontaneously (i.e., $\Delta G_{\text{net}} < 0$) under control condition *i*. The calculations of ΔG_{net} for conditions *ii*, *iii*, *v*, and *vi* are made at the instant the external solution change is made.

‡ Conditions *ii*, *iii*, *v*, and *vi* are given for the instant at which the external solution change is made, assuming that V_1 has had time to shift, but that all other intracellular parameters are unaltered from the previous steady state.

0 mM, the basolateral membrane instantly hyperpolarizes by ~ 40 mV; V_1 is assumed to be -30 mV. The initial ΔG_{net} is $-0.7RT$, which predicts a continued HCO_3^- efflux. However, $J_{\text{HCO}_3}^{\text{net}}$ is only $-5.5P$, which predicts that this efflux should be reduced by two-thirds compared with the control. Thus, this model cannot account for the observed fall of pH_i (i.e., efflux of HCO_3^- or an equivalent species) unless there is a concomitant change in P . (*vi*) When $[\text{Na}^+]_b$ is restored to 100 mM, the basolateral membrane initially hyperpolarizes, usually to beyond -100 mV. Assuming V_1 is -100 mV and $[\text{HCO}_3^-]_i$ is 2.8 mM, the initial ΔG_{net} is $-2.7RT$, which predicts a net HCO_3^- efflux, not the influx required to explain the observed rise of pH_i. $J_{\text{HCO}_3}^{\text{net}}$ comes to $-10.4P$, which predicts that the HCO_3^- efflux should be sizeable.

CL-HCO₃ EXCHANGE For an electroneutral Cl-HCO₃ exchanger, the net change in free energy is:

$$\Delta G_{\text{net}} = RT \ln \frac{[\text{HCO}_3^-]_b [\text{Cl}^-]_i}{[\text{HCO}_3^-]_i [\text{Cl}^-]_b}$$

where a negative value for ΔG_{net} indicates net Cl⁻ influx and HCO₃⁻ efflux. Activities are understood in place of concentrations. It is possible to calculate ΔG_{net} for the same six conditions as above, during changes in either [HCO₃⁻]_b or [Na⁺]_b. (i) Under standard control conditions (see Table VI), the values for a_b^{Cl} and a_i^{Cl} are ~71 and 16 mM, respectively. Thus, ΔG_{net} is $-1.0RT$, and HCO₃⁻ would leave the cell in exchange for Cl⁻. This model would therefore account for the sustained fall in pH_i observed after applying CO₂/HCO₃⁻ Ringer (Fig. 1A). (ii) When [HCO₃⁻]_b is reduced from 10 to 2 mM, ΔG_{net} rises to $-2.6RT$. Thus, if anything, HCO₃⁻ efflux would increase, consistent with the observed pH_i decrease. However, a_i^{Cl} should rise in proportion to the net intracellular alkali loss, which was not observed, as noted in the analysis of Fig. 5. (iii) When [HCO₃⁻]_b is returned to 10 mM, a_i^{Cl} starts off at ~19 mM. The initial ΔG_{net} is $0.0RT$, which predicts no net HCO₃⁻ flux. Therefore, the Cl-HCO₃ exchange model cannot account for the rise of pH_i, presumably caused by the net influx of HCO₃⁻ or an equivalent species, which occurs upon raising [HCO₃⁻]_b. (iv) In the new control condition in which [Na⁺]_i is 0 mM, a_i^{Cl} is assumed to be 16 mM. ΔG_{net} comes to $-1.0RT$, which predicts a net efflux of HCO₃⁻ (or an equivalent species). As noted in the Results, the data of Fig. 7B are consistent with a slowing or a reversal of the net HCO₃⁻ efflux. (v) At the instant [Na⁺]_b is reduced to 0 mM, there are no changes in any of the relevant activities, and ΔG_{net} remains at $-1.0RT$, predicting a net HCO₃⁻ efflux unchanged from the control state. Thus, this model cannot account for the observed rapid fall in pH_i. (vi) Just before [Na⁺]_b is restored to 100 mM, a_i^{Cl} is ~20 mM. The ΔG_{net} , at the instant [Na⁺]_b is raised, is no different from that value prevailing immediately before the [Na⁺]_b increase, $0.0RT$. Thus, this model predicts no net HCO₃⁻ flux, and therefore cannot account for the observed, rapid rise of pH_i.

NA-H EXCHANGE IN PARALLEL WITH CL-HCO₃ EXCHANGE For an electroneutral, basolateral Na-H exchanger, the net change in free energy is:

$$\Delta G_{\text{net}} = RT \ln \frac{[\text{Na}^+]_i [\text{H}^+]_b}{[\text{Na}^+]_b [\text{H}^+]_i}$$

where a negative value for ΔG_{net} indicates net Na⁺ influx and H⁺ efflux. The free energy change for a Cl-HCO₃ exchanger is given above. (i) In the standard control condition with 100 mM Na⁺ in the lumen (see Table VI), ΔG_{net} (Na-H) is $-1.6RT$, whereas, as pointed out above, ΔG_{net} (Cl-HCO₃) is $-1.0RT$. The net effect of the parallel operation of the two exchangers is net Na⁺ and Cl⁻ influx, and net H⁺ and HCO₃⁻ efflux. If the transport rates of the two exchangers were fortuitously identical, the net result would be isohydric NaCl influx; such a mechanism has previously been postulated for the luminal membrane (Liedtke and Hopfer, 1977). If, on the other hand, the two rates were not identical, the net effect of the two transport processes would be either an increase or a decrease in pH_i. (ii) When [HCO₃⁻]_b is reduced from 10 to 2 mM, the instantaneous ΔG_{net} (Na-H) becomes zero, whereas ΔG_{net} (Cl-HCO₃) increases to $-2.6RT$. Thus, for this experimental maneuver, the parallel exchangers would behave as would a single Cl-HCO₃ exchanger (see CL-HCO₃ EXCHANGE above). (iii) At the instant [HCO₃⁻]_b is restored to 10 mM, ΔG_{net} (Na-H) becomes $-2.6RT$, whereas ΔG_{net} (Cl-HCO₃) becomes zero. Thus, for condition iii, the parallel exchangers would behave as a single Na-H exchanger. However, our pH_i recovery data indicate

a rate constant approximately twice as great as that expected for pure Na-H exchange. Furthermore, the pH_i recovery was only inhibited about half by 2 mM amiloride, a treatment which should have eliminated 80% of Na-H exchange. (iv) In the new control condition with $[\text{Na}^+]_i = 0$ mM, a_i^{Na} is ~ 11 mM (Sackin et al., 1981). Thus, ΔG_{net} (Na-H) across the basolateral membrane is $-2.4RT$, and ΔG_{net} (Cl-HCO₃) is $-1.0RT$. This condition is similar to *i* above with respect to net Na⁺ and Cl⁻ gain and the effect on pH_i . (v) When $[\text{Na}^+]_b$ is also reduced to 0 mM, the instantaneous ΔG_{net} (Na-H) becomes $+\infty$, whereas ΔG_{net} (Cl-HCO₃) is unchanged at $-1.0RT$. Thus, there would be a Cl⁻ gain and a Na⁺ loss combined with a fall in pH_i , secondary to both H⁺ gain and HCO₃⁻ loss. These predictions qualitatively agree with our data. (vi) Just before $[\text{Na}^+]_b$ is restored to 100 mM, a_i^{Na} is ~ 2.5 mM (Sackin et al., 1981). At the instant $[\text{Na}^+]_b$ is raised, ΔG_{net} (Na-H) is $-4.7RT$ and ΔG_{net} (Cl-HCO₃) is zero. Thus, the parallel exchanger hypothesis predicts that pH_i should recover because of Na-H exchange alone. Our data, however, contradict this prediction on three counts: first, the rate constant of the pH_i recovery exceeds that for pure Na-H exchange; second, the recovery is sensitive to SITS; and third, the pH_i recovery is HCO₃⁻ dependent.

NA/HCO₃-CL/H EXCHANGE The predicted free energy change is:

$$\Delta G_{\text{net}} = RT \ln \frac{[\text{Na}^+]_i [\text{HCO}_3^-]_i [\text{Cl}^-]_b [\text{H}^+]_b}{[\text{Na}^+]_b [\text{HCO}_3^-]_b [\text{Cl}^-]_i [\text{H}^+]_i}$$

where a negative value for ΔG_{net} indicates a net influx of Na⁺ and HCO₃⁻, and a net efflux of Cl⁻ and H⁺. (i) Under standard control conditions (see Table VI), ΔG_{net} is $-0.6RT$, which predicts a net uptake of Na⁺ and HCO₃⁻, and a net loss of Cl⁻ and H⁺. This is opposite to the expected net HCO₃⁻ efflux, based on the sustained fall in pH_i which accompanies application of CO₂/HCO₃⁻ Ringer (Fig. 1A). (ii) When $[\text{HCO}_3^-]_b$ is reduced to 2 mM, the initial ΔG_{net} is $+2.6RT$. This correctly predicts a net Na⁺ and HCO₃⁻ efflux. It also implies an absolute dependence on Cl⁻, as well as a net Cl⁻ influx which should amount to half of the total alkali efflux plus acid influx. Our data, however, do not support these last two predictions. In the first place, an absolute dependence on Cl⁻ was not observed when Cl⁻ was replaced by cyclamate, glucuronate, or sulfate in the $[\text{HCO}_3^-]_b$ reduction experiments. Second, concomitant change in a_i^{Cl} did not have a time course and magnitude consistent with the changes in pH_i and a_i^{Na} . (iii) At the instant $[\text{HCO}_3^-]_b$ is restored to 10 mM, ΔG_{net} becomes $-2.5RT$, which correctly predicts a net uptake of Na⁺ and HCO₃⁻. It also predicts a dependence on Cl⁻ as well as a Cl⁻ efflux, which are not supported by our data (see *ii* above). (iv) In the new control condition in which $[\text{Na}^+]_i$ is zero, ΔG_{net} is $-1.4RT$, which predicts a net uptake of Na⁺ and HCO₃⁻, and a net loss of Cl⁻ and H⁺. The predicted pH_i change is thus not inconsistent with the data of Fig. 7B, which indicates that the net HCO₃⁻ efflux should be slowed or even reversed. (v) When $[\text{Na}^+]_b$ is reduced to zero, ΔG_{net} becomes $+\infty$, correctly predicting a net Na⁺ and HCO₃⁻ efflux. This model also predicts an absolute dependence on Cl⁻ as well as a simultaneous uptake of Cl⁻, which should amount to half the total alkali leaving plus acid entering the cell. The Cl⁻ dependence was not observed, and, as pointed out in Results, both the time course and the magnitude of the a_i^{Cl} increase were inappropriate. (vi) At the instant $[\text{Na}^+]_b$ is restored to 100 mM, ΔG_{net} becomes $-4.7RT$, which correctly predicts a net influx of Na⁺ and HCO₃⁻. However, this model also predicts an absolute requirement for Cl⁻ as well as a simultaneous efflux of Cl⁻, which should amount to half the total alkali gained plus acid lost from the cell. The Cl⁻ dependence was not observed, and, as pointed out in Results, both the time course and magnitude of the a_i^{Cl} decrease were inappropriate.

ELECTROGENIC NA/HCO₃ TRANSPORT The models *e1-e4* are thermodynamically equivalent. Their common predicted free energy change, when expressed in the form for model *e1*, is:

$$\Delta G_{\text{net}} = RT \ln \frac{[\text{Na}^+]_b [\text{HCO}_3^-]_b^2}{[\text{Na}^+]_i [\text{HCO}_3^-]_i^2} + FV_1,$$

where a negative value for ΔG_{net} signifies net Na⁺ and equivalent HCO₃⁻ efflux. (*i*) Under standard control conditions (Table VI), this model predicts $\Delta G_{\text{net}} = -0.3RT$. The efflux of HCO₃⁻ thus predicted is consistent with the sustained fall in pH_i observed after application of CO₂/HCO₃⁻ Ringer. (*ii*) Reducing [HCO₃⁻]_b from 10 to 2 mM would bring ΔG_{net} to $-2.7RT$, which predicts an increase in both Na⁺ and HCO₃⁻ efflux, consistent with the d_i^{Na} and pH_i data. (*iii*) When [HCO₃⁻]_b is returned to 10 mM, ΔG_{net} becomes $+1.45RT$. This would probably produce an influx of both Na⁺ and HCO₃⁻, once again consistent with the data. (*iv*) In the new control condition when [Na⁺]_i is 0 mM, ΔG_{net} is very slightly positive, $+0.1RT$. This is consistent with the earlier explanation for the pH_i changes of Fig. 7B, in which we pointed out that removing luminal Na⁺ would slow or even reverse the electrogenic Na/HCO₃ system. (*v*) Reducing [Na⁺]_b to zero in the absence of luminal Na⁺ causes a substantial basolateral depolarization and causes ΔG_{net} to approach $-\infty$, favoring net Na⁺ and HCO₃⁻ efflux. This is consistent with the observed fall of pH_i. (*vi*) When [Na⁺]_b is returned to 100 mM, V_1 reaches -100 mV, causing ΔG_{net} to rise to $+2.0RT$, favoring net Na⁺ and HCO₃⁻ uptake. These predictions are also consistent with the d_i^{Na} and pH_i data.

We gratefully acknowledge the technical assistance of Mr. Jeffrey B. Hughes.

This work was supported by Public Health Service Research Grant 5-R01-AM-13844 and Program Project AM-17433 from the National Institute of Arthritis, Diabetes, Digestive and Kidney Diseases. W. Boron was supported, for part of the time, by National Research Service Award GM-06499.

Received for publication 16 February 1982 and in revised form 17 August 1982.

REFERENCES

- ANAGNOSTOPOULOS, T., and G. PLANELLES. 1979. Organic anion permeation at the proximal tubule of *Necturus*. *Pflügers Arch. Eur. J. Physiol.* **381**:231-239.
- BORON, W. F., and E. L. BOULPAEP. 1981a. Intracellular pH regulation in salamander renal proximal tubule. *Kidney Int.* **19**:233. (Abstr.)
- BORON, W. F., and E. L. BOULPAEP. 1981b. Basolateral bicarbonate transport in isolated, perfused renal proximal tubules of the salamander. *Fed. Proc.* **40**:356. (Abstr.)
- BORON, W. F., and E. L. BOULPAEP. 1982. Hydrogen and bicarbonate transport by salamander proximal tubule cells. In *Intracellular pH: Its Measurement, Regulation, and Utilization in Cellular Function*. R. Nuccitelli and D. Deamer, editors. Liss, New York. 253-267.
- BORON, W. F., and E. L. BOULPAEP. 1983. Intracellular pH regulation in the renal proximal tubule of the salamander: Na-H exchange. *J. Gen. Physiol.* **81**:29-52.
- BORON, W. F., W. C. MCCORMICK, and A. ROOS. 1979. pH regulation in barnacle muscle fibers: dependence on intracellular and extracellular pH. *Am. J. Physiol.* **237**:C185-C193.
- BORON, W. F., W. C. MCCORMICK, and A. ROOS. 1981. pH regulation in barnacle muscle fibers: dependence on extracellular sodium and bicarbonate. *Am. J. Physiol.* **240**:C80-C89.
- BURCKHARDT, B.-CH., and E. FRÖMTER. 1980. Bicarbonate transport across the peritubular

- membrane of rat kidney proximal tubule. *In* Hydrogen Ion Transport in Epithelia. I. Schulz, G. Sachs, J. G. Forte, and K. J. Ullrich, editors. Elsevier/North-Holland, Amsterdam. 277–285.
- FRÖMTER, E. 1975. Electrophysiological studies on the mechanism of H^+/HCO_3^- transport in rat kidney proximal tubule. *In* Proc. Int. Congr. Nephrol. 6th ed. Firenze. 25–26. (Abstr.)
- GARRELS, R. M., M. E. THOMPSON, and R. SIEVER. 1961. Control of carbonate solubility by carbonate complexes. *Am. J. Sci.* **259**:24–45.
- GOLDMAN, D. 1943. Potential, impedance and rectification in membranes. *J. Gen. Physiol.* **27**:37–60.
- GUGGINO, W. B., E. L. BOULPAEP, and G. GIEBISCH. 1980. The mechanisms of chloride transport across the basolateral membrane of the *Necturus* proximal tubule. *Kidney Int.* **19**:135A. (Abstr.)
- GUGGINO, W. B., E. L. BOULPAEP, and G. GIEBISCH. 1982. Electrical properties of chloride transport across the *Necturus* proximal tubule. *J. Membr. Biol.* **65**:185–196.
- HODGKIN, A. L., and B. KATZ. 1949. The effect of sodium ions on the electrical activity of the giant axon of the squid. *J. Physiol. (Lond.)* **198**:37–77.
- KIMURA, G., and K. R. SPRING. 1979. Luminal Na^+ entry into *Necturus* proximal tubule cells. *Am. J. Physiol.* **236**:F295–F301.
- KINSELLA, J. L., and P. S. ARONSON. 1980. Properties of the Na^+-H^+ exchanger in renal microvillus membrane vesicles. *Am. J. Physiol.* **238**:F461–F469.
- LIEDTKE, C. M., and U. HOPFER. 1977. Anion transport in brush border membranes isolated from rat small intestine. *Biochem. Biophys. Res. Commun.* **76**:579–585.
- MURER, H., U. HOPFER, and R. KINNE. 1976. Sodium/proton antiport in brush-border-membrane vesicles isolated from rat small intestine and kidney. *Biochem. J.* **154**:597–604.
- RADTKE, H. W., G. RUMRICH, E. KINNE-SAFRAN, and K. J. ULLRICH. 1972. Dual action of acetazolamide and furosemide on proximal volume absorption in the rat kidney. *Kidney Int.* **1**:100–105.
- ROOS, A., and W. F. BORON. 1981. Intracellular pH. *Physiol. Rev.* **61**:296–434.
- RUSSELL, J. M., and W. F. BORON. 1982. Intracellular pH regulation in squid giant axons. *In* Intracellular pH: Its Measurement, Regulation, and Utilization in Cellular Function. R. Nuccitelli and D. Deamer, editors. Liss, New York. 221–237.
- SACKIN, H., W. F. BORON, and E. L. BOULPAEP. 1981. Intracellular sodium activity in *Ambystoma* renal proximal tubule. *Kidney Int.* **19**:255. (Abstr.)
- SACKIN, H., and E. L. BOULPAEP. 1981a. The isolated, perfused salamander proximal tubule: methods, electrophysiology and transport. *Am. J. Physiol.* **241**:F39–F52.
- SACKIN, H., and E. L. BOULPAEP. 1981b. Isolated perfused salamander proximal tubule. II. Monovalent ion replacement and rheogenic transport. *Am. J. Physiol.* **241**:F540–F555.
- SACKIN, H., A. B. MAUNSBACH, and E. L. BOULPAEP. 1982. Correlation between basolateral membrane electrical resistance and ultrastructure in isolated perfused renal proximal tubules. *Kidney Int.* **21**:286.
- SPRING, K. R., and G. KIMURA. 1978. Chloride reabsorption by renal proximal tubules of *Necturus*. *J. Membr. Biol.* **38**:233–254.
- STEELE, P. S., and E. L. BOULPAEP. 1976. Effect of pH on ionic conductances of the proximal tubule epithelium of *Necturus* and the role of buffer permeability. *Fed. Proc.* **35**:465. (Abstr.)
- THOMAS, R. C. 1970. New design for sodium-sensitive glass microelectrode. *J. Physiol. (Lond.)* **210**:82P–83P.
- THOMAS, R. C. 1974. Intracellular pH of snail neurones measured with a new pH-sensitive glass microelectrode. *J. Physiol. (Lond.)* **238**:159–180.

- THOMAS, R. C. 1977. The role of bicarbonate, chloride and sodium ions in the regulation of intracellular pH in snail neurones. *J. Physiol. (Lond.)* **273**:317-338.
- ULLRICH, K. J., G. CAPASSO, G. RUMRICH, F. PAPAVALASSIOU, and S. KLÖSS. 1977. Coupling between proximal tubular transport processes. Studies with ouabain, SITS and HCO_3^- -free solutions. *Pflügers Arch. Eur. J. Physiol.* **368**:245-252.
- ULLRICH, K. J., H. W. RADTKE, and G. RUMRICH. 1971. The role of bicarbonate and other buffers on isotonic fluid absorption in the proximal convolution of the rat kidney. *Pflügers Arch. Eur. J. Physiol.* **330**:149-161.
- ULLRICH, K. J., G. RUMRICH, and K. BAUMANN. 1975. Renal proximal tubular buffer-(glycodiazine) transport. Inhomogeneity of local transport rate, dependence on sodium, effect of inhibitors and chronic adaptation. *Pflügers Arch. Eur. J. Physiol.* **357**:149-163.
- WARNOCK, D. G., and F. C. RECTOR, JR. 1979. Proton secretion by the kidney. *Annu. Rev. Physiol.* **41**:197-210.